OSMOTICALLY INDUCED TRANSLOCATION OF ΔN-TRPV1 CHANNELS IN SUPRAOPTIC NEURONS

A Thesis Submitted to the College of
Graduate and Postdoctoral Studies
In Partial Fulfillment of the
Requirements for the Degree of
Master of Science
In the Department of
Anatomy, Physiology, and
Pharmacology
University of Saskatchewan
Saskatoon

By

Kirk D. Haan

PERMISSION TO USE

In presenting this thesis in partial fulfilment of the requirements for a Postgraduate degree from the University of Saskatchewan, I agree that the Libraries of this University may make it freely available for inspection. I agree that permission for copying of this thesis in any manner, in whole or in part, for scholarly purposes may be granted by the professor or professors who supervised my thesis work or, in their absence, by the Head of the Department or the Dean of the College in which my thesis work was completed. It is understood that any copying or publication or use of this thesis or parts thereof for financial gain shall not be allowed without my written permission. It is also understood that due recognition shall be given to me and to the University of Saskatchewan in any scholarly use which may be made of any material in my thesis.

Requests for permission to copy or to make other use of material in this thesis in whole or part should be addressed to:

Dean of Graduate and Postdoctoral Studies

University of Saskatchewan

116 Thorvaldson Building

110 Science Place

Saskatoon, Saskatchewan, S7N 5C9

Canada

ABSTRACT

The physiological mechanisms involved in regulating extracellular osmolality are critical to understand how mammals cope with dehydration and water deprivation. Osmoregulation is a crucial homeostatic process in mammals that functions to maintain a physiological setpoint of extracellular osmolality. Magnocellular neurosecretory cells (MNCs) of the hypothalamus sense changes in external osmolality and transduce changes in cell volume into depolarizing currents and action potential (AP) firing, leading to the release of the hormone vasopressin (VP), which prevents water loss from the kidneys. MNCs lack the normal volume regulatory mechanisms present in other cells, and possess mechanosensitive channels called ΔN-TRPV1 that enable cation influx and MNC plasma membrane depolarization upon activation by cell shrinkage that involves a Ca^{2+}-dependent isoform of the enzyme phospholipase C (PLC) called PLCδ1. Sustained exposure (i.e., longer than 1 hour) to high osmolality causes structural and functional adaptations in MNCs, like somatic hypertrophy, channel translocation, and changes in gene expression. We propose a potential mechanism for MNC hypertrophy and for osmotically induced ΔN-TRPV1 translocation in MNCs that may provide insight into the underlying mechanisms of long-term MNC osmoregulation. Isolated MNCs treated with hyperosmotic saline for 1 hour elicited somatic hypertrophy as well as a significant increase in the number of ΔN-TRPV1 channels present on the plasma membrane. Both the increase in plasma membrane ΔN-TRPV1 and MNC hypertrophy were shown to be reversible once isolated MNCs were returned to isosmotic solution. The increase in plasma membrane ΔN-TRPV1 and hypertrophy were observed to be PLC- and protein kinase C (PKC)-dependent, and both required SNARE-mediated exocytosis and movement of vesicles from the Golgi, as inhibitors of PLC, PKC, the SNARE complex, and the Golgi all prevented the osmotically induced increase in plasma membrane ΔN-TRPV1 as well as hypertrophy. It was also

observed that the retrieval of ΔN-TRPV1 from the plasma membrane as well as the recovery from hypertrophy require dynamin-mediated endocytosis, as using an inhibitor of dynamin prevented the retrieval of ΔN-TRPV1 from the plasma membrane and the recovery from hypertrophy. Finally, we report that mice that lack PLCδ1 fail to elicit an increase in plasma membrane ΔN-TRPV1 or hypertrophy in response to high external osmolality, suggesting that this enzyme is necessary for these processes. This project will help to elucidate the potential mechanisms underlying osmosensory transduction and osmoregulation in MNCs.

ACKNOWLEDGEMENTS

This thesis is a representation of my work as both an undergraduate Honour's student and MSc. candidate in the department of Anatomy, Physiology and Pharmacology at the University of Saskatchewan. Throughout my tenure I have learned a great deal about what it means to participate in research and to work with integrity and diligence. Learning how to work with initiative and properly design and implement experimental protocols has potentiated my growth as a scientist, as a student, and as a person. There are many who have guided me in this journey, and I would like to take the proper time to give each their due respect.

I would first like to thank my supervisor, Dr. Thomas E. Fisher. His continuous support, guidance, and mentorship have been invaluable to me, and I have grown immensely as a student, as a researcher, and as a person, thanks to him. I would certainly not be where I am today personally or professionally without him. I have learned a great deal about what a true mentor and leader look like from him. Finally, I would like to thank Dr. Fisher for the various references he has provided for me, as well as for the opportunity to design my own experimental protocol and for teaching me how to write manuscripts for publication.

I would next like to thank my wonderful committee members, Dr. Veronica Campanucci and Dr. John Howland. I sincerely appreciate their time and efforts in helping me succeed, and I have learned so much from both of them in the multiple classes I have taken of theirs in my undergraduate and graduate degrees, as well as for encouraging me to expand my knowledge in academics and in life. I would like to thank Dr. Suraj Unniappan for kindly agreeing to be the external examiner for my thesis.

I would also like to thank my fellow laboratory members, Dr. Sung Jin Park and Mr. Xuan Thanh Vo. I have learned an incredible amount about conducting research and writing papers from Sung Jin, and he has been an outstanding mentor for me. Xuan's unbroken patience throughout my time in the laboratory has been invaluable to me. He has been at the forefront of helping me develop my techniques, and I would certainly not be where I am today without his technical guidance.

Finally, I would like to thank Dr. Quentin Greba. Though he is not part of my laboratory, he has been a tremendous help in teaching me how to perform a rat transcardial perfusion, discussing certain research protocols with me, and has given me insight into how to improve the efficacy and efficiency of my experiments.

I would like to acknowledge that this project was funded by the University of Saskatchewan APP Devolved Graduate Funding Scholarship. The operations funding for this project also were provided in part by a Natural Sciences and Engineering Research Council (NSERC) Discovery Grant and by a College of Medicine Bridge Funding Grant.

TABLE OF CONTENTS

LIST OF FIGURES

LIST OF ABBREVIATIONS

Ang II	Angiotensin II
AQP	Aquaporin channel
AP	Action potential
AT_1R	Angiotensin type-1 receptor
BAPTA-AM	1,2-Bis(2-aminophenoxy)ethane-N,N,N',N'-tetraacetic acid tetrakis (acetoxymethyl ester)
Ca^{2+}	Calcium ion
$[Ca^{2+}]_i$	Intracellular calcium concentration
cAMP	3'-5' cyclic adenosine monophosphate
CCD	Cortical collecting duct
Cl^-	Chlorine ion
CSA	Cross-sectional area
DAG	Diacylglycerol
ECF	Extracellular fluid
GABA-AR	γ-aminobutyric acid type-a receptor
GLUT	Glutamate
GPCR	G protein-coupled receptor
H^+	Hydrogen ion
HCO_3^-	Carbonate ion
ICF	Intracellular fluid
IP_3	Inositol 1,4,5-triphosphate

K^+	Potassium ion
κOR_1	κ-opioid receptor-1
MNC	Magnocellular neurosecretory cell
MnPO	Median preoptic nucleus
mosmol kg^{-1}	Milliosmoles per kilogram of solvent
mosmol L^{-1}	Milliosmoles per litre of solvent
MT	Microtubules
Na^+	Sodium ion
NKCC	Sodium-Potassium-Chloride cotransporter
NMDAR	N-methyl-D-aspartate receptor
NSF	*N*-ethylmaleimide sensitive fusion protein
OVLT	Organum vasculosum of the lamina terminalis
OT	Oxytocin
PBS	Phosphate-buffered solution
PBST	Phosphate-buffered solution containing Triton X-100
PFA	Paraformaldehyde
PGC	PIPES-glucose-calcium chloride buffer solution
PIP_2	Phosphatidylinositol 4,5-bisphosphate
PIPES	Piperazine-N,N'-bis(2-ethanesulfonic acid)
PKC	Protein kinase C
PLC	Phospholipase C
PP	Posterior pituitary
PVN	Paraventricular nucleus

RMP	Resting membrane potential
RTK	Receptor tyrosine kinase
RVD	Regulatory volume decrease
RVI	Regulatory volume increase
SEM	Standard error of the mean
SFO	Subfornical organ
SNARE	Soluble NSF attachment protein receptor
SON	Supraoptic nucleus
TRP	Transient receptor potential channel
TRPV	Transient receptor potential vanilloid channel
ΔN-TRPV1	N-terminal splice variant of the TRPV1 channel
VGCC	Voltage-gated calcium channel
VP	Vasopressin
VR_{1a}	Vasopressin type-1a receptor
VR_2	Vasopressin type 2 receptor

CHAPTER 1: INTRODUCTION

1.1 Osmolality, osmolarity, and osmoregulation

Solutions comprised of solute and solvent possess physical properties that depend on the relative amounts of each, which are referred to as colligative properties (Pinarbasi et al., 2009). These properties include freezing point, boiling point, vapour pressure, and osmotic pressure (Voet et al., 2000). In cellular physiology the most important colligative property is osmotic pressure (Sanger et al., 2001), which is defined as, "the minimum pressure that must be applied to a solution in order to prevent inward flow of solvent across a semi-permeable membrane" (Voet et al., 2000). When two solutions comprised of different solute concentrations are separated by a semi-permeable membrane, water will move across the membrane from the solution with a lower solute concentration to the solution with a higher solute concentration through passive diffusion, which is known as osmosis (Voet et al., 2000). In living organisms with a selectively permeable cell membrane, osmosis occurs between the extracellular fluid (ECF) and intracellular fluid (ICF). In multicellular organisms, the relevant solutes in the ECF and ICF that dictate osmosis are mainly electrolytes (e.g., ions), but organic molecules (e.g., proteins, hormones, neurotransmitters) can also influence osmosis (Fleischhaur et al., 1995). The ICF is comprised of the cellular cytosol and is also known as the fluid of the internal environment of a cell (Luby-Phelps, 1999). The ECF consists of both the interstitial fluid (i.e., the fluid in between cells) and the blood plasma (e.g., the noncellular component of blood; Gauer et al., 1970). It is critical to maintain fluid and electrolyte balance within an organism (Rolls and Phillips, 1990), and the maintenance and regulation of both fluid and electrolyte balance are accomplished at the cellular level, as well as the organ level

(Sawka and Montain, 2000). The renal system is a chief regulator of fluid and electrolyte balance in mammals (Bankir et al., 1989). At the cellular level the plasma membrane is key to this balance, which is accomplished by specialized pores and channels in the plasma membrane that allow water and ions to passively move between the ICF and ECF (Curran and Solomon, 1957). Osmolality is a measurement that calculates the moles of osmolytes (e.g., ions, proteins, or other small organic molecules) present per kilogram of solvent and is expressed in the units of osmoles per kilogram (osmol kg^{-1}), or more commonly in mammals, in milliosmoles per kilogram (mosmol kg^{-1}). Osmolarity is an analogous measurement that is often mistaken for osmolality. Although the two terms measure the moles of osmolyte per amount solvent, osmolarity indicates the moles of osmolyte per litre of solvent instead of per kilogram of solvent and is expressed using osmoles per litre (osmol L^{-1}) or milliosmoles per litre (mosmol L^{-1}; Erstad, 2003).

Some aquatic animals possess the ability to change the osmolality of their internal environment based on the osmolality of their external environment through optimized cell volume regulatory mechanisms and are therefore termed osmoconformers because of their ability to conform to the osmolality of whatever environment they are present in (Bourque, 2008). Mammals, however, must regulate the osmolality of their internal environment, and maintain a range of osmolalities close to a physiological "setpoint" (usually around 300 mosmol kg^{-1}; Bourque, 2008). Mammals are therefore termed osmoregulators for their requirement to constantly regulate their internal osmolality (Bourque, 2008). ECF osmolality within a certain range in mammals (usually within 10 mosmol kg^{-1}) is deemed isosmotic to the animal. ECF osmolality lower than normal is deemed hypoosmotic, while ECF osmolality higher than the normal range is deemed hyperosmotic. When ECF osmolality changes, water flows through the cell membrane via osmosis, which maintains

osmotic equilibrium between the ICF and ECF (Halperin and Skorecki, 1986; Bourque, 2008), with the difference in osmolality between the two compartments being the driving force for osmotic pressure that enables osmosis to occur (Guyton and Hall, 2006; Boron and Boulpaep, 2017). In the ECF the most important ion present is sodium (Na^+; Terry, 1994) and regulating Na^+ and water levels is the primary regulatory process mammals utilize to maintain isosmotic ECF osmolality (Guyton and Hall, 2006; Bourque, 2008). Na^+ regulation occurs through changes in Na^+ appetite (Weisinger et al., 1983; Blackburn et al., 1993) and changes in the rate of Na^+ excretion (i.e., natriuresis; Huang et al., 1996). Water levels are regulated through thirst, sweating, evaporation, and urine output (Verney, 1947; Zerbe and Robertson, 1983; Fortney et al., 1984; Tucker, 1968; Bourque, 2008). Behaviourally, high serum osmolality from dehydration triggers thirst in mammals and the desire to drink water to alleviate the osmotic stress on the body (Maresh et al., 2001; Smith et al., 2004). Urine output is also decreased under hyperosmolar conditions (Bourque, 2008). In situations of over-hydration, in which ECF osmolality becomes hypoosmotic, thirst and salt appetite are decreased, and urine output is increased to restore the ECF osmolality to isosmotic levels (Bourque, 2008). ECF hyperosmolality causes cells to shrink due to water moving from ICF to ECF through water pores until osmotic equilibrium is restored, while ECF hypoosmolality causes cellular swelling due to water moving into the cell (Lang et al., 1998; Lang, 2007; Chamberlin and Strange, 1989). Many cells possess cell volume regulatory mechanisms to respond to these changes in cell volume. Shrinkage due to hyperosmolality will activate ion channels that will move solutes into the cell from the extracellular fluid (ECF) in order to restore osmotic balance (Lang 2007; Lang et al., 1998). Among these ion channels are: the NKCC1 cotransporter, the Na^+/H^+ antiporter, and the HCO_3^-/Cl^- antiporter (Lang 2007; Grinstein and Foskett, 1990). NKCC1 causes the influx of Na^+, K^+, and 2 Cl^-; the Na^+/H^+ antiporter brings Na^+

into the cell while expelling H^+, and the HCO_3^-/Cl^- exchanger brings Cl^- into the cell while expelling HCO_3^- (Lang et al., 1998; Lang 2007; Boron and Boulpaep, 2017). The H^+ and HCO_3^- form H_2O and CO_2 outside the cell, which then passively diffuse into the cell due to the increase in ions from the transporters mentioned above (Lang 2007; Boron and Boulpaep, 2017). As the ion and water concentrations return to an equilibrium, the cell returns to its original volume. This response to cell shrinkage is known as *regulatory volume increase* (RVI; Lang et al., 1998). The opposite occurs in response to hypoosmolality, where cellular swelling inactivates the channels that increase their basal activity during RVI and activates K^+ and Cl^- leak channels as well as a K^+/Cl^- cotransporter in order to expel K^+ and Cl^- ions into the ECF (Lang et al., 1998; Lang 2007; Boron and Boulpaep, 2017). H_2O then passively follows the ion flow out of the cell and the cell returns to its original volume. The response to cell swelling is also known as *regulatory volume decrease* (RVD; Lang et al., 1998). The maintenance and close regulation of ECF osmolality is essential for mammals, especially in the brain, where large changes in cell volume could potentially damage the brain parenchyma (Bourque, 2008). The structural integrity and health of this tissue is imperative to proper organismal function and survival, and severe damage can lead to neuronal misfiring, hyper- or hypo-excitability, and neuronal death (Bourque, 2008).

1.2 Osmoreceptors

1.2.1 Osmoreceptor function

Osmoregulation is a crucial homeostatic process in mammals that functions to maintain a physiological setpoint of serum osmolality (Zerbe and Robertson, 1983). Because mammals are

sensitive to changes in ECF osmolality, they must closely regulate their internal environments. This is accomplished largely through osmoreceptors, which are unique cells specifically designed to detect changes in ECF osmolality and activate mechanisms throughout the body to cope with these changes and restore ECF osmolality (Bourque, 2008). These osmoreceptors are largely present in the brain and are the chief regulators of osmotic homeostasis in mammals (Jewell and Verney, 1957; Verney, 1947). Many years of research have led to the conclusion that the physiological setpoint of ECF osmolality is determined by osmoreceptor electrical activity (Bourque, 2008). The resting membrane potential (RMP) of a cell is defined as the electrical potential difference across a cell membrane of an excitable cell at rest (Hodgkin and Huxley, 1952). In osmoreceptors, RMP is influenced by membrane stretch, which can then be transduced to changes in ion channel activity, thereby changing the electrical potential difference across a cell membrane and therefore the cell's excitability (Verney, 1947; Hodgkin and Huxley, 1952; Bourque, 2008). Changes in ECF osmolality therefore change the excitability of osmoreceptors, which then changes their likelihood to fire action potentials (APs; Bourque, 2008).

1.2.2 Anatomy and morphology

Many of the cerebral osmoreceptors are located in the organum vasculosum of the lamina terminalis (OVLT; Thrasher et al., 1982) and in the subfornical organ (SFO; Anderson et al., 2000), which are anatomically located, respectively, on the ventral and dorsal surfaces of the third ventricle (Morita et al., 2004; Egan et al., 2003). These primary osmoreceptors sense changes in extracellular fluid (ECF) osmolality and adjust their firing rate (Bourque and Oliet, 1997; Bourque et al., 1994). These primary osmoreceptors project to other osmoreceptors through the median

preoptic nucleus (MnPO) to neurons located in the supraoptic nucleus (SON; Oliet and Bourque, 1992; Oliet and Bourque, 1993; Bourque et al., 1994) and paraventricular nucleus (PVN; Qiu et al., 2004) and release glutamate (GLUT) to enhance the activity of the neurons in these nuclei. The SON and PVN possess a specialized type of osmoreceptor known as a magnocellular neurosecretory cell (MNC; Oliet and Bourque, 1992; Qiu et al., 2004). MNCs in the SON are mostly surrounded by other MNCs, but astrocytes (Tweedle and Hatton, 1977; Theodosis and Poulain, 1984) and some interneurons (Hatton, 1990) are also present. These neurons also possess a singular axon (Brownstein et al., 1980) and between 1 and 3 dendrites (Stern and Armstrong, 1998). The dendrites primarily project to the surrounding glia (Armstrong et al., 1982), while MNC axons project mostly to the posterior pituitary (PP; Brownstein et al., 1980). MNCs located in the SON and PVN have 2 subtypes: vasopressin (VP)- synthesizing, and oxytocin (OT)- synthesizing (Swaab et al., 1975; Sofroniew, 1982; Bicknell, 1988). There is also some evidence for the presence of peripheral osmoreceptors located in the stomach (Carlson et al., 1997) and the liver (Baertschi and Vallet, 1981), but the focus of this thesis will be on central osmoreception.

1.2.3 Neurohypophysial hormones and hormonal release

VP is a neuroendocrine hormone synthesized in MNC cell bodies that is packaged into synaptic vesicles and then moved down a singular axon through the median eminence where it is then released from axon terminals located in the PP (Brownstein et al., 1980; Bicknell, 1988). Hormonal release from axon terminals occurs when an AP reaches a terminal, depolarizes the surrounding membrane, and activates voltage-gated Ca^{2+} channels (VGCCs; Hatton, 1990; Armstrong, 1995), which leads to Ca^{2+} influx and subsequent exocytosis of vesicles containing VP (or OT) into the

general circulation through the blood plexus located in the PP (Hatton, 1990; Armstrong, 1995). VP release from MNCs can also occur without AP firing through a phenomenon known as quantal release (Roper et al., 2004), but the majority of AP release requires APs. Once in the general circulation, VP travels to the kidneys and binds to vasopressin-2 receptors (VR_2) located on epithelial cells of the cortical collecting duct (CCD) in the distal nephron (Agre, 2006: Petersen, 2006: Ball, 2007). The binding of VP to VR_2 promotes water reabsorption through insertion of specialized water channels called aquaporin-2 (AQP_2) into the apical membrane of CCD epithelial cells via cyclic adenosine monophosphate (cAMP)-dependent translocation (Knepper et al., 2015; Agre, 2006: Peterson, 2006: Ball, 2007). The basolateral membrane of the CCD epithelial cells also possesses AQP_3 and AQP_4 which also aids in water reabsorption (Agre, 2006: Peterson, 2006: Ball, 2007). In the brain, it has been shown that VP also helps maintain cellular water and salt balance through AQP modulation on astrocyte membranes (Niermann et al., 2001). MNCs can also release VP from dendrites to surrounding astrocytes, which has been thought to play a role in regulating MNC function (Ludwig, 1998).

OT is a neuroendocrine hormone that is largely involved in promoting childbirth and lactation in females (Moon and Turner, 1959; Guyton and Hall, 2006), and sperm motility and testosterone production in males (Studdard et al., 2002; Gupta et al., 2008), but is also involved in inhibiting salt appetite (Blackburn et al., 1993; Blackburn et al., 1995). In the brain, OT functions to influence a variety of behaviours, including sexual arousal (Murphy et al., 1987; Blaicher et al., 1999) and personal attachment (Fineberg and Ross, 2017). OT also possesses a natriuretic role in rodents (Verbalis et al., 1991). OT-MNCs have also been shown to be osmosensitive and respond to

changes in cell volume (Wakerly et al., 1978). OT release from MNCs increases with progressive dehydration (Wakerly et al., 1978; Marzban et al., 1992).

MNCs at rest fire 1-3 APs per second (Poulain and Wakerly, 1982), which corresponds to a small amount of hormone being released from the axon terminal. However, hyperosmotic stimulation can rapidly enhance AP firing from MNCs (Poulain and Wakerly, 1982), which enhances subsequent hormone release. At a certain level of hyperosmotic stimulation, MNCs switch to a phasic firing pattern, which is a specific type of burst firing in which a high frequency of APs is fired followed by a period of rest (Dutton and Dyball, 1979; Bicknell and Leng, 1981). This firing pattern has shown to be the most effective for rapid hormone release from axon terminals in both VP- and OT-MNCs (Dutton and Dyball, 1979; Bicknell and Leng, 1981; Andrew and Dudek, 1984). These observations showed that the firing pattern of MNCs can change to meet the demand for hormone release (Bicknell, 1988). OT-MNCs also display shorter and faster phasic firing patterns than VP-MNCs (Wakerly et al., 1978).

1.2.4 MNC activity

MNCs are specialized neurons in the SON and PVN that detect changes in external osmolality (Bourque et al., 2007; Bourque, 2008). Changes in external osmolality change MNC membrane potential, thereby affecting the ability to fire APs and therefore also affecting VP and OT release (Oliet and Bourque, 1992; Bourque, 2008; Bicknell, 1988). MNCs transduce decreases in cell volume caused by increases in external osmolality into depolarizing currents via mechanosensitive channels (Oliet and Bourque, 1993), which increases the likelihood of MNC action potential (AP)

firing in response to excitatory inputs coming from osmoreceptors in the OVLT and SFO (Bourque and Oliet, 1997). Increases in osmolality as little as 3 mosmol kg^{-1} can significantly enhance MNC AP firing (Poulain and Wakerly, 1982; Bourque and Oliet, 1997). This can then lead to the downstream release of VP into the PP and therefore enhance water reabsorption at the kidneys to prevent further increases in osmolality from occurring (Robertson et al., 1976). The mechanosensitive channels that mediate the transduction of cell volume changes into depolarizing currents are inactivated by increases in membrane tension (i.e., membrane expansion; Oliet and Bourque, 1993; Bourque, 2008). Under hypoosmotic conditions MNCs swell and the mechanosensitive channels close, which leads to a decrease in depolarizing current, and under hyperosmotic conditions MNCs shrink and the mechanosensitive channels open, leading to an increase in depolarizing current (Oliet and Bourque, 1993; Bourque, 2008). Depriving rats of water for 24 hours also enhances L-type Ca^{2+} current in MNCs (Zhang et al., 2007a). ΔN-TRPV1 channels in MNCs interact with the cytoskeleton, and it is thought that the force exerted onto the channels by the cytoskeleton in response to changes in external osmolality triggers the opening or closing of the channel. The mechanosensitivity of MNCs involves actin filaments as well as microtubules (MTs; Zhang et al., 2007b; Prager-Khoutorsky et al., 2014). These molecules have been hypothesized to also be involved in regulating mechanosensitive ion channel activity in MNCs during osmoregulation (Prager-Khoutorsky et al., 2014; Prager-Khoutorsky and Bourque, 2015; Prager-Khoutorsky, 2017).

1.2.5 ΔN-TRPV1 in MNCs

The transient receptor potential (TRP) family of channels is a group of non-selective cation channels that have multiple subtypes and subfamilies with widespread expression throughout the nervous system (Montell, 2001). The TRP vanilloid (TRPV) subfamily are expressed in multiple types of excitable cells like neurons (Montell, 2001; Montell, 2005) and are known to be sensitive to heat and capsaicin (Caterina et al., 1997). The TRPV1 channel is an important contributor to neuronal depolarization as it is a nonselective cation channel (Kedei et al., 2001; Clapham, 2003) that is permeable to Ca^{2+}, Na^{+}, and K^{+}. An N-terminal variant of the TRPV1 channel has been identified in MNCs and is now known as ΔN-TRPV1 (Sharif-Naeini et al., 2006; Zaelzer et al., 2015). ΔN-TRPV1 is a mechanosensitive channel, meaning it is stretch-gated and is influenced by changes in cell volume (Prager-Khoutorsky et al., 2014; Prager-Khoutorsky and Bourque, 2015). ΔN-TRPV1 is mechanically linked to the cytoskeleton through connections with MTs (Prager-Khoutorsky et al., 2014; Prager-Khoutorsky and Bourque, 2015). Disrupting the mechanical linkage between MTs and ΔN-TRPV1 prevents increases in MNC firing under osmotic stress (Prager-Khoutorsky et al., 2014; Prager-Khoutorsky and Bourque, 2015). Actin also plays a role in mediating ΔN-TRPV1 mechanosensitivity (Zhang et al., 2007b; Prager-Khoutorsky and Bourque, 2015). Osmotically evoked filamentous actin (F-actin) polymerization enhances the mechanical gating of ΔN-TRPV1 (Zhang et al., 2007b), which could possibly occur through regulation of mechanical plasma membrane support (Prager-Khoutorsky, 2017). The exact mechanism of the actin- ΔN-TRPV1 interaction remains elusive. MNCs express a unique MT scaffold that enables them to transduce changes in cell volume into depolarizing currents through physical interactions with ΔN-TRPV1 (Prager-Khoutorsky et al., 2014). ΔN-TRPV1

mechanosensitivity is also influenced by interactions with subcortical actin (Prager-Khoutorsky and Bourque, 2015; Prager-Khoutorsky, 2017). When there is a disruption in the MT scaffold or in the subcortical actin that can lead to the dissociation of either MTs or actin, MNCs lose the ability to transduce changes in cell volume into depolarizing currents (Prager-Khoutorsky et al., 2014; Prager-Khoutorsky and Bourque, 2015; Prager-Khoutorsky, 2017). MT dissociation also prevents osmotically induced increases in ΔN-TRPV1 current and MNC osmosensory transduction from occurring (Prager-Khoutorsky et al., 2014), suggesting that the ΔN-TRPV1-cytoskeleton interaction is integral to transducing osmotically evoked changes in MNC cell volume into depolarizing currents that can increase the likelihood of AP firing and therefore VP release.

1.3 Osmotic Adaptations

1.3.1 Short-term adaptations

MNCs are able to respond quickly to changes in osmolality and modulate their electrical and physiological activity accordingly (Bourque et al., 1994; Zhang and Bourque, 2003; Bourque, 2008). These changes in osmolality lead to the opening of ion channels, which causes changes in cellular conductance (Bourque et al., 2002) Conductance is the ability of a cell to move ions across the cell membrane (Baxter and Byrne, 1991). The change in electrical activity is mediated by ΔN-TRPV1 channels (Zaelzer et al., 2015). All cells rapidly shrink when exposed to hyperosmotic solution (Lang et al., 1998). In MNCs the decrease in membrane tension that occurs as a result of membrane shrinkage when exposed to hyperosmotic solution activates ΔN-TRPV1 channels and promotes cation influx, depolarization, AP firing, and downstream VP release (Bourque, 2008;

Zaelzer et al., 2015). The opposite occurs in response to a decrease in external osmolality; MNCs swell, membrane tension increases, and ΔN-TRPV1 inactivates, resulting in hyperpolarization, decreased AP firing and decreased VP release (Bourque, 2008; Zaelzer et al., 2015). The increase in VP release from MNCs in response to high osmolality is a clever mechanism that mammals have developed to enhance water reabsorption and prevent further increases in external osmolality from occurring (Bourque, 2008). Hyperosmotic or hypoosmotic exposure caused rapid shrinkage or swelling, respectively, in both hippocampal neurons and in MNCs (Zhang and Bourque, 2003). Cells were exposed to either hyperosmotic or hypoosmotic solution for up to 14 minutes (Zhang and Bourque, 2003). MNCs displayed a more dramatic and longer-lasting shrinkage or swelling than did hippocampal neurons (Zhang and Bourque, 2003). MNCs remained shrunk or swollen as long as the osmotic stressor was present, while hippocampal neurons rapidly returned to close to their original volume through RVI and RVD (Zhang and Bourque, 2003). This finding suggested that MNCs do not possess the cell volume regulatory processes present in most other cell types (e.g., the mechanisms described in section 1.1; Zhang and Bourque, 2003). Because MNCs are osmoreceptors and rely on changes in cell volume and membrane tension to transduce changes in external osmolality into depolarizing currents, the lack of normal volume regulatory mechanisms has been suggested to allow mechanosensitive ΔN-TRPV1 channels to transduce the changes in external osmolality into those depolarizing currents in order to enhance AP firing and VP release (Zhang and Bourque, 2003; Zaelzer et al., 2015).

1.3.1.1 Phospholipase C

Phospholipase C (PLC) is a key enzyme involved in multiple intracellular processes in multiple cell types (Rhee, 2001). PLC cleaves phosphatidylinositol 4,5-bisphosphate (PIP_2) into inositol triphosphate (IP_3) and diacylglycerol (DAG; Rhee, 2001). IP_3 enhances Ca^{2+} release from intracellular stores like the endoplasmic reticulum (Rhee, 2001). DAG is an important second messenger that remains in the cytoplasm and activates the enzyme protein kinase C (PKC; Rhee, 2001). PKC is a versatile phosphorylating enzyme with a variety of intracellular functions including modulating channel translocation and protein expression (Bell, 1986; Premkumar and Ahern, 2000; Vellani et al., 2001; Strong et al., 1987). In addition to being a precursor molecule for IP_3 and DAG, PIP_2 is known to be involved in ion channel regulation (Suh and Hille, 2008), and to interact with the cytoskeleton (Raucher et al., 2000; Logan and Mandato, 2006).

Many families of PLC exist, but the 3 most well-studied families are PLCβ, PLCγ, and PLCδ, which each possess distinct mechanisms of activation and requirements for activation that are specific to their function within the cell (Rohacs et al., 2008; Rohacs, 2013). PLCδ is the most poorly understood of these isoform families (Rebecchi and Pentyala, 2000), but it is known to require an increase in intracellular Ca^{2+} ($[Ca^{2+}]_i$) for full activation (Allen et al., 1997; Rohacs et al., 2008). PLCδ isoforms are the most sensitive to small changes in $[Ca^{2+}]_i$ (Allen et al., 1997; Rohacs et al., 2008). PLCβ isoforms are activated by interactions with the G$\beta\gamma$ or Gqα subunits of G-protein coupled receptors (GPCRs; Rebecchi and Pentyala, 2000; Rohacs et al., 2008). PLCγ isoforms are activated by adjacent receptor tyrosine kinases (RTKs), which act as receptors for hormones like insulin (Rebecchi and Pentyala, 2000; Rohacs et al., 2008). These isoforms are

expressed in brain tissue including the SON (Suh et al., 1988; Lee et al., 1999; Suh et al., 2008). The PLCδ isoforms are primarily stimulated by intracellular Ca^{2+} (Essen et al., 1996), and are expressed in MNCs (Allen et al., 1997; Fukami et al., 2001; Hazell et al., 2012). PLCδ1 and PLCδ4 isoforms have been identified in MNCs (Hazell et al., 2012; Nakamura and Fukami, 2017). PLCδ1 is the most Ca^{2+}-sensitive PLCδ isoform (Suh et al., 1988; Lee et al., 1999). The physiological role of the PLCδ family is well-understood in other cell types such as keratinocytes and cardiac myocytes, but its role in neurons remains poorly understood (Kadamur and Ross, 2013; Nakamura and Fukami, 2017).

1.3.1.2 Angiotensin II

Angiotensin II (Ang II) is a peptide hormone that possesses a variety of functions in the body, including increasing blood pressure, Na^+ reabsorption, and VP release (Fyhrquist et al., 1995; Jhamandas et al., 1989; Buggy et al., 1979; Qadri et al., 1993). It is synthesized largely outside the brain (Bie et al., 2004), but within brain tissue it is synthesized and released from osmoreceptors in the OVLT and SFO and provides excitatory input to MNCs in the SON and PVN (Renaud et al., 1983; Jhamandas et al., 1989; Li and Ferguson, 1993). Ang II is released from the OVLT and SFO in response to systemic hypovolemia or hypernatremia, both of which involve an increase in ECF osmolality (Jhamandas et al., 1989; Li and Ferguson, 1993). Ang II binds to the angiotensin type-1 receptor (AT_1R) present on MNC cell bodies (Morris et al., 1999) and potentiates MNC sensitivity to changes in external osmolality (Chakfe and Bourque, 2000). The modulation of MNC mechanosensitivity by Ang II occurs through interactions with PLC and PKC (Zhang et al., 2007b; Zhang and Bourque, 2008; Prager-Khoutorsky and Bourque, 2010). Isolated MNCs exposed to

Ang II exhibited enhanced cortical F-actin polymerization (Zhang et al., 2007b) and TRPV1 open probability (Zhang and Bourque, 2008). These events occur in a PLC-dependent manner in MNCs (Zhang et al., 2007b; Zhang and Bourque, 2008; Prager-Khoutorsky and Bourque, 2010).

1.3.2 Long-term adaptations

Mammals are able to adapt to long-term water deprivation and dehydration through behavioural mechanisms as well as through neurohormonal mechanisms that involve MNCs (Bourque, 2008). This can be examined *in vivo* by depriving rats of water for periods of days (Modney and Hatton, 1989; Wakerly et al., 1982). These adaptations can also be studied *in vitro* by exposing isolated MNCs to solutions of varying osmolalities and observing the responses (Shah et al., 2014). MNC adaptations are sustained as long as the stressor is present and are reversed when the stressor is removed, and involve both structural and functional adaptations (Hatton, 1997), as well as changes in gene expression and membrane density of channels and receptors (Shuster et al., 1999; Tanaka et al., 1999; Hurbin et al., 2002).

1.3.2.1 Structural adaptations

MNCs in the SON and the surrounding glia undergo structural changes that potentially contribute to sustained hormone release during sustained increases in external osmolality (Hatton, 1997). Under normal homeostatic conditions about 1% of MNCs in the SON are in direct membranous contact with other MNCs (Tweedle and Hatton, 1977; Modney and Hatton, 1989). However, during periods of dehydration MNC-MNC contact can increase to about 10% and is reversible

with rehydration (Tweedle and Hatton, 1976; Tweedle and Hatton, 1977; Gregory et al., 1980). The increase in MNC-MNC contact coincides with increases in the size of the SON under long-term hyperosmotic stress (Tweedle and Hatton, 1976; Tweedle and Hatton, 1977; Gregory et al., 1980). Increases in blood osmolality from dehydration cause glial retraction in the SON and PP, and MNC somatic hypertrophy (Modney and Hatton, 1989; Marzban et al., 1992). Long-term hyperosmotic stress lasting days can lead to glial retraction in the SON and PP as well as enlargement of MNCs in the SON (Modney and Hatton, 1989; Marzban et al., 1992). In rats that were subjected to a 10-day dehydration period via drinking hyperosmotic water, there was about a 170% increase in the size of their SONs compared to hydrated rats (Modney and Hatton, 1989). Capacitance represents the capacity of charge separation of a cell and is dependent on the plasma membrane surface area (Hille, 2001; Partridge and Partridge, 2003), and can be continually measured in cells and is used to understand membrane dynamics under stressors like either hypoosmotic or hyperosmotic shock (Rhoades and Bell, 2009; Boron and Boulpaep, 2017). When hippocampal neurons were exposed to either a hyperosmotic or hypoosmotic solution, they displayed respective increases or decreases in capacitance (Zhang and Bourque, 2003). Exposure to hyperosmotic or hypoosmotic stress for 14 minutes did not result in a change in capacitance in MNCs (Zhang and Bourque, 2003). However, a 33% increase in membrane capacitance was observed in the MNCs of rats that were progressively dehydrated by drinking salt water for 7 days (Tanaka et al., 1999). Another study by Shah et al., (2014) found that 90-minute hyperosmotic exposure resulted in a 7% increase in MNC capacitance. These studies suggest that acute osmotically evoked changes in MNC size are not associated with changes in membrane capacitance, but sustained exposure to hyperosmolality can lead to changes in MNC membrane capacitance. Another study examined changes in MNC structure under hypoosmotic conditions in

rats and found that a 7-day hypoosmotic challenge through pharmacological inhibition of urine production led to a 40% decrease in both somatic area and nuclear size (Verbalis and Drutarosky, 1988; Zhang et al., 2001). These findings examined together suggest that MNCs possess the ability to structurally adapt and change their cell size in response to both hyperosmotic and hypoosmotic stressors (Hatton, 1997; Zhang et al., 2001; Bourque, 2008). In a study conducted by Beagley and Hatton (1992) rats were injected with hyperosmotic saline, and their MNCs were examined 5 hours after injection. There was a significant increase in MNC size, suggesting that MNC hypertrophy occurs within hours (Beagley and Hatton, 1992). Another study by Shah et al., (2014) observed MNC hypertrophy *in vitro* after 90-minute hyperosmotic stimulation of isolated MNCs, which will be discussed in more detail in section 1.5.1.

1.3.2.2 Functional adaptations

MNCs also adapt functionally under osmotic stress through the enhanced membrane density of different membrane receptors and ion channels (Glasgow et al., 2000; Burbach et al., 2001; Yue et al., 2006; Shuster et al., 1999; Tanaka et al., 1999). The changes in protein density are hypothesized to enable MNCs to fire APs more rapidly to sustain a high level of hormonal release (e.g., VP) to cope with sustained increases in external osmolality (Glasgow et al., 2000; Burbach et al., 2001; Yue et al., 2006; Hatton, 1997). Changes in protein expression and gene upregulation contribute to the functional adaptations of MNCs in response to sustained increases in external osmolality (Glasgow et al., 2000; Burbach et al., 2001; Yue et al., 2006). The movement of channels and receptors from the cytoplasm to the MNC membrane through translocation is another adaptation present in MNCs (Tanaka et al., 1999; Shuster et al., 1999).

1.3.2.3 Changes in MNC plasma membrane channel and receptor presence

Mammals that are subjected to dehydration for periods lasting multiple days adjust to the increased need for water conservation through multiple mechanisms (Robertson et al., 1976; Hurbin et al., 2002). MNCs respond by enhancing VP production and release to conserve water at the kidneys (for more information on VP, see section 1.2.3; Bourque, 2008). There is an increase in MNC plasma membrane vasopressin-1a receptor (VR_{1a}) levels in response to dehydration (Hurbin et al., 2002). The increase in membrane bound VR_{1a} is due to a process called translocation (Hurbin et al., 2002). Translocation is a process by which ion channels and membrane receptors are inserted into the plasma membrane (Teruel and Meyer, 2000), and is described in further detail in section 1.4.3. Stimulating VR_{1a} on MNCs can also lead to an increase in MNC firing and an increase in plasma membrane VR_{1a} density via translocation (Hurbin et al., 2002).

Na^+ channels translocate to the plasma membrane and increase electrical activity in MNCs in response to progressive dehydration (Tanaka et al., 1999). The increase in membrane Na^+ channel density and open probability decreases the threshold for AP firing and contributes to enhanced MNC activity (Tanaka et al., 1999). MNCs therefore possess the adaptive ability to change their intrinsic electrical properties in response to hyperosmotic stress (i.e., dehydration; Tanaka et al., 1999).

High osmolality increases MNC plasma membrane κ-opioid receptor levels (Shuster et al., 1999). Intraperitoneal injections of hyperosmotic saline were given to mice, and MNCs were isolated from SONs 60 minutes after injection (Shuster et al., 1999). The mice injected with hyperosmotic

saline had increased the amount of κ-opioid receptor-1 (κOR_1) present on the MNC plasma membrane compared to the MNCs of mice that were not injected with hyperosmotic saline (Shuster et al., 1999). The amount of plasma membrane κOR_1 in the hyperosmotic-injected mice was also higher than the amount of κOR_1 associated with the membranes of intracellular vesicles in MNCs, suggesting osmotically induced translocation of κOR_1 to the plasma membrane occurs in MNCs in response to exposure to hyperosmotic saline (Shuster et al., 1999). Dynorphin is an endogenous opioid peptide that is known to stimulate κOR_1 (Chavkin et al., 1982). In supraoptic neurons dynorphin can be packaged in the same vesicles as VP (Whitnall et al., 1983), which can be released from the dendrites and axon terminals of MNCs (Pow and Morris, 1989). Dynorphin and VP that are released from MNC dendrites decreases Ca^{2+} influx and neuropeptide release (Brown and Bourque, 2004; Brown and Bourque, 2006). The combination of dynorphin release and increase in membrane κOR_1 density in MNCs results in autocrine regulation of MNC firing to promote phasic firing of MNCs under hyperosmotic stress, which helps control VP and OT release (Shuster et al., 1999; Brown and Bourque, 2004; Brown and Bourque, 2006).

1.3.2.4 Changes in protein expression in MNCs

In addition to enhancing VP production, dehydration also increases VR_{1a} mRNA levels and synthesis of new VR_{1a} in MNCs (Hurbin et al., 2002). Increasing water load (i.e., lowering body osmolality) decreases VP production, VR_{1a} mRNA levels, and VR_{1a} synthesis in MNCs (Hurbin et al., 2002). The co-expression of VP and its autoreceptor, VR_{1a}, suggests that the nuclear pathways that result in their synchronized regulation are interconnected or similar (Hubrin et al.,

2002), and that changes in VR_{1a} levels and VP are important in the long-term functional adaptations of MNCs.

A slower increase in Na^+ channel expression (i.e., the synthesis of new Na^+ channels) was also shown to occur in MNCs after animals were injected with hyperosmotic saline (Tanaka et al., 1999). The increase in Na^+ channel expression suggests that it is part of a longer-term response of MNCs to high osmolality and helps MNCs to then insert new Na^+ channels into the membrane when needed (Tanaka et al., 1999).

1.4 Exocytosis, endocytosis, and translocation

Exocytosis and endocytosis are two fundamentally important processes in cellular physiology (Ceccarelli et al., 1973; Heuser and Reese, 1981). Exocytosis is a process by which cytoplasmic vesicles fuse with the plasma membrane (Ceccarelli et al., 1973). A vesicle that will undergo exocytosis may contain contents within its membrane to be expelled (e.g., wastes or neurotransmitters), or contain channels or receptors incorporated into its membrane to then be fused with the plasma membrane (Chen and Scheller, 2001). Empty vesicles also undergo exocytosis and fuse with the plasma membrane (Chen and Scheller, 2001). Endocytosis is a process that brings molecules or substances (e.g., nutrients, proteins, or foreign pathogens) into the cell for further processing or degradation, or returning membrane proteins into vesicles (Pastan and Willingham, 1985). Because both processes are essential for cellular survival there are multiple mechanisms by which they occur (Miaczynska and Stenmark, 2008; Battey et al., 1999), with the most common form of exocytosis being through the soluble N-ethylmaleimide sensitive

factor attachment protein receptor (SNARE)-mediated exocytosis (Chen and Scheller, 2001; Zorec, 2018), and the most common form of endocytosis being clathrin/dynamin-mediated endocytosis (Battey et al., 1999; Raimondi et al., 2011).

1.4.1 SNARE-mediated exocytosis

SNARE-mediated exocytosis of channels contained in intracellular vesicles is an evolutionary mechanism in neurons designed to minimize the delay in transmission between pre- and post-synaptic sites (Sabatini and Regehr, 1999). SNARE is a complex that involves a variety of proteins present at or near the intracellular plasma membrane or on the vesicle, including SNAP25, synaptobrevin, synaptotagmin, syntaxin, N-methylmaleimide sensitive factor (NSF), α-SNAP, and n-Sec-1 (Zorec, 2018; Montana et al., 2009). Intracellular Ca^{2+} signals intracellular vesicles containing the proteins synaptotagmin and synaptobrevin to travel to the membrane (Zorec, 2018; Boron and Boulpaep, 2017). Once at the membrane, n-Sec-1 dissociates from syntaxin and allows synaptobrevin to attach and form a complex together with itself and SNAP-25 (Zorec, 2018; Boron and Boulpaep, 2017). This complex is known as the SNARE complex. Once the complex is formed, α-SNAP and NSF attach to the complex (Zorec, 2018). Ca^{2+} influx triggers the vesicle to begin to fuse with the membrane by binding to synaptotagmin, but fusion will not occur without ATP hydrolysis by the ATPase NSF (Vivona et al., 2013). Once ATP hydrolysis occurs via NSF the vesicle fuses with the membrane (Vivona et al., 2013).

Fast synaptic neurotransmission involves the rapid translocation of synaptic vesicles from the axon terminal to the membrane, where the vesicles fuse with the membrane and release their contents

(e.g., neurotransmitters) onto effector cells like neurons and muscle fibers (Vivona et al., 2013). Synaptic neurotransmission requires higher $[Ca^{2+}]_i$ in the terminal to initiate translocation and is extremely rapid (Boron and Boulpaep, 2017). This fast type of SNARE-mediated exocytosis involves synaptotagmin isoforms that are less Ca^{2+}-sensitive to enable more rapid translocation and release of neurotransmitter for neuronal communication, as the exocytotic machinery is present near the plasma membrane and can detect the rapid influx of Ca^{2+} coming from nearby L-type Ca^{2+} channels (Boron and Boulpaep, 2017). For example, MNCs receive input from osmoreceptors in the OVLT and SFO through synaptic neurotransmission and the release of neurotransmitters like GLUT to rapidly transmit osmosensory information (Bourque et al., 1994). This rapid transmission enables MNCs to then enhance their sensitivity to changes in external osmolality and adjust their firing rate and hormone release accordingly (Bourque et al., 1994).

Hormone release is generally a slower process than synaptic transmission (Boron and Boulpaep, 2017). It requires higher $[Ca^{2+}]_i$ than synaptic transmission, but occurs over a longer period of time (Zorec, 2018; Boron and Boulpaep, 2017). The slow Ca^{2+} buildup is sensed by synaptotagmin isoforms that are more Ca^{2+}-sensitive and are located further away from the plasma membrane (Zorec, 2018; Boron and Boulpaep, 2017). Hormone release is an endocrine response that involves release of hormones into the blood to travel to an effector cell or organ and therefore does not require the immediate response that synaptic transmission requires (Boron and Boulpaep, 2017). For more information on hormone release in MNCs see section 1.2.3.

SNARE-mediated exocytosis can also be modulated by second messenger pathways like the PLC pathway (Zorec, 2018; Segovia et al., 2010). This type of SNARE-mediated exocytosis is a slower

process than hormonal release and can be used for the translocation and incorporation of channels and receptors to the plasma membrane (Zorec, 2018; Boron and Boulpaep, 2017). PKC activation by PLC enables PKC to phosphorylate parts of the SNARE complex and promotes translocation of vesicles to the plasma membrane as well as fusion of vesicles with the plasma membrane (Camprubí-Robles et al., 2009; Montana et al., 2009). In nociceptors, noxious (painful) stimuli promote SNARE-mediated insertion of TRPV1 channels in a PKC-dependent manner to the cell body membrane in order to enhance depolarization and likelihood of AP firing, thereby enhancing nociceptor sensitivity to the noxious stimuli (Camprubí-Robles et al., 2009). PKC activation influences the translocation and the exocytosis of certain receptors and channels and is involved in the functional adaptations of neurons (Strong et al., 1987; Morgan and Burgoyne, 1992; Newton, 2001; Morenilla-Palao et al., 2004; Camprubí-Robles et al., 2009; Planells-Cases et al., 2011).

1.4.2 Dynamin-mediated endocytosis

Dynamin is a chief mediator of cellular endocytosis (Shpetner and Vallee, 1989; Koenig and Ikeda, 1989). It is a GTPase that is involved in modulating the amount of clathrin present on the external cell membrane (Damke et al., 1994; Vallis et al., 1999) and is essential for internal membrane fission for vesicle and receptor internalization (Henley et al., 1998). Multiple isoforms of dynamin exist (Raimondi et al., 2011), with dynamin-1 being expressed in the highest concentration in neurons (Nakata et al., 1991; Ferguson et al., 2007). Dynamin senses membrane indentation and polymerizes into helices around the newly formed endocytic bud where GTPase activity is increased (Ford et al., 2011). It then promotes membrane fission and therefore release of the newly formed internalized vesicle into the cell (Liu et al., 2011).

1.4.3 Translocation and neuronal modulations

Somatic translocation is a dynamic and reversible process that involves the movement of channels and receptors to the plasma membrane from internal stores (Teruel and Meyer, 2000). SNARE-mediated exocytosis is the primary method of membrane insertion for these translocated channels and receptors (Teruel and Meyer, 2000; Zorec, 2018). Some receptors and channels are internalized when a stimulus is removed and they are no longer required on the plasma membrane (Vieira et al., 1996; Carroll et al., 2001; Henley et al., 1998). This can occur through mechanisms like dynamin-mediated endocytosis (Henley et al., 1998; Morenilla-Palao et al., 2004; Camprubí-Robles et al., 2009). During neurotransmitter release, the depolarization caused by the AP that reaches the axon terminal triggers Ca^{2+} influx through VGCCs and signals synaptic vesicles that are docked at the plasma membrane to fuse with the membrane, releasing their contents onto effector cells (Hatton, 1990; Armstrong, 1995), usually through SNARE-mediated exocytosis (Pryer et al., 1992; Rothman, 1994; Sudhof, 1995). In the cell body a variety of ion channels and receptors translocate to the plasma membrane when a stimulus is presented to the neuron (Wan et al., 1997; Lan et al., 2001; Jeske et al., 2009; Morenilla-Palao et al., 2004; Planells-Cases et al., 2011). Exogenous stimulation can stimulate translocation of γ-aminobutyric acid-A receptors (GABA-ARs; Wan et al., 1997) and N-methyl-D-aspartate receptors (NMDARs; Lan et al., 2001). Stimulation with certain growth factors like nerve growth factor (NGF) can stimulate translocation of ion channels like TRPC5 and TRPC3 (Clapham, 2003; Singh et al., 2004) as well as TRPV1 (Jeske et al., 2009). Neuronal translocation aids functional adaptations of neurons to facilitate phenomena like neuronal plasticity, electrical excitability and sensitivity to exogenous stimuli (Burgoyne and Morgan, 1993; Cocucci et al., 2006).

The ability of certain receptors and ion channels to translocate to the membrane when needed and to be internalized when not needed is a functional adaptation of cells like neurons to be able to cope with a constantly changing external environment (Carroll et al., 2001; Cocucci et al., 2006; Boron and Boulpaep, 2017). TRPV1 translocation specifically is essential in nociceptors and sensory neurons to enhance the neuronal sensitivity to noxious and sensory stimuli, respectively (Morenilla-Palao et al., 2004; Camprubí-Robles et al., 2009; Planells-Cases et al., 2011; Jeske et al., 2009). In response to noxious stimuli TRPV1 will translocate to nociceptor plasma membranes to enhance the ability of the nociceptor to fire APs to transmit the information about the noxious stimuli in order to enhance a retractive and protective response from the organism (Morenilla-Palao et al., 2004; Camprubí-Robles et al., 2009). When the noxious stimulus is removed, TRPV1 will be internalized and the nociceptor will return to its basal firing state (Morenilla-Palao et al., 2004; Camprubí-Robles et al., 2009). In MNCs, somatic translocation of various ion channels, receptors, and neurocrine molecules influence the sensitivity of MNCs to changes in osmolality (Shuster et al., 1999; Tanaka et al., 1999; Brown and Bourque, 2004; Bourque, 2008).

1.5 Recent evidence for the role of PLCδ1 in MNC osmoregulation

The current focus of our laboratory's research is on the structural adaptations of MNCs under hyperosmotic stress. We use a combination of electrophysiology and biochemical assays like immunocytochemistry and immunohistochemistry for *in vitro* experimentation to understand more clearly the underlying mechanisms behind MNC osmoregulation. Our laboratory recently

developed a protocol to examine MNC hypertrophy in isolated cells (Shah et al., 2014), as many potential aspects of MNC hypertrophy are difficult to study *in vivo*.

The enhancement of water reabsorption by VP enables animals to endure longer periods without water, which enhances survivability in situations where water may not be readily available days or weeks (Knepper et al., 2015). The opening of ΔN-TRPV1 channels in MNCs in response to sustained increases in osmolality can aid in enhancing AP firing and hormone output, but how or whether these currents are integrated with MNC hypertrophy are unknown. It is possible that in addition to the increase in ΔN-TRPV1 conductance there is an increase in the number of ΔN-TRPV1 channel density on the MNC plasma membrane during sustained increases in osmolality that were inserted through translocation. The mechanisms that govern short-term osmoregulation may also be involved in the long-term responses, but the increase in ion channel density, gene expression, and MNC size in response to sustained hyperosmolar exposure suggests that there may be additional mechanisms responsible for the long-term adaptations of MNCs to hyperosmolality that enable sustained high levels of AP firing and hormone release.

1.5.1 Evidence for the mechanisms of hypertrophy in isolated MNCs

Shah et al., (2014) observed hypertrophy in isolated MNCs. This study involved exposing isolated MNCs to hyperosmotic solution for 90 minutes, instead of periods of days of dehydration that were used for the *in-situ* experiments previously described (Modney and Hatton, 1989). It is important to note, however, that the increase in cell size observed *in vitro* was modest (107% compared to control; Shah et al., 2014) compared to the hypertrophy observed *in situ* (170%

compared to control; Modney and Hatton, 1989). In addition to observing MNC hypertrophy *in vitro*, they showed that MNC hypertrophy was also dependent on APs, Ca^{2+} influx through L-type Ca^{2+} channels, increases in $[Ca^{2+}]_i$, TRPV1 currents, PLC, and PKC, as performing the experiment in the presence of blockers of these parameters prevented hypertrophy (Shah et al., 2014). They also tested whether exocytosis and endocytosis were respectively required for the initiation and reversal of hypertrophy by performing the experiment in the presence of an inhibitor of the SNARE complex as well as a dynamin inhibitor and found that blocking SNARE-mediated exocytosis prevented hypertrophy from occurring, and that blocking dynamin-mediated endocytosis prevented the recovery from hypertrophy (Shah et al., 2014). They also examined plasma membrane PIP_2 concentrations and found that hyperosmotic triggered a decrease in PIP_2 immunofluorescence (Shah et al., 2014). These findings led our laboratory to hypothesize that PLC and PKC are both required for MNC hypertrophy, and that hyperosmotic stimulation alone could trigger PLC activation.

1.5.2 The role of a Ca^{2+}-dependent PLC isoform in osmotically evoked ΔN-TRPV1 currents

A study by our laboratory in 2017 showed that the osmotically evoked increase in ΔN-TRPV1 currents in isolated MNCs requires Ca^{2+}. Similar to a previous study by our laboratory (Shah et al., 2014), they examined PIP_2 immunofluorescence in isolated MNCs under different experimental conditions. They found that hyperosmotic stimulation or the addition of the Ca^{2+} ionophore A-23187 to isosmotic solution resulted in a decrease in PIP_2 immunofluorescence, while inhibiting PLC using U-73122 or removing Ca^{2+} using BAPTA-AM in hyperosmotic solution prevented the decrease in PIP_2 immunofluorescence, suggesting that Ca^{2+} alone could activate PLC

(Bansal and Fisher, 2017). Next, they examined the effects of the known PLC activator Ang II on PIP_2 immunofluorescence and osmotic activation (for more information on Ang II and its connection to PLC, see section 1.3.1.2). Isolated MNCs in isosmotic solution were exposed to Ang II, which resulted in a decrease in PIP_2 immunofluorescence (Bansal and Fisher, 2017). When PLC activation by Ang II was combined with hyperosmotic stimuli, there was no additional increase in PIP_2 immunofluorescence from administering these treatments separately (Bansal and Fisher, 2017). This observation suggested that osmotic activation of PLC and PLC activation by Ang II may depend on the same intracellular pathways (Bansal and Fisher, 2017). Lastly, isolated MNCs in isosmotic solution were exposed to the PLC activator m-3M3FBS and a similar decrease in PIP_2 immunofluorescence was observed (Bansal and Fisher, 2017), suggesting that the mechanisms underlying osmotic PLC activation are similar to the mechanisms by which Ang II activates PLC (Bansal and Fisher, 2017). To examine the effects of PLC and PKC on baseline and osmotically evoked ΔN-TRPV1 currents they first exposed isolated MNCs in isosmotic solution to a PKC activator (phorbol 12-myristate 13-acetate) and found that it increased basal ΔN-TRPV1 currents as well as osmotically evoked ΔN-TRPV1 currents when a hyperosmotic solution was added (Bansal and Fisher, 2017). Osmotic activation of PLC via a hyperosmotic solution enhanced ΔN-TRPV1 activity while PLC inhibition by U-73122 reduced osmotically evoked ΔN-TRPV1 currents in isolated MNCs (Bansal and Fisher, 2017). PKC inhibition by GF-109203 also reduced osmotically evoked ΔN-TRPV1 currents in MNCs (Bansal and Fisher, 2017). They suggested that because osmotically evoked PLC requires Ca^{2+}, and ΔN-TRPV1 currents are decreased by PLC inhibition, MNCs potentially express a Ca^{2+}-dependent PLC pathway that is activated by MNC depolarization and Ca^{2+} influx through L-type Ca^{2+} channels (Bansal and Fisher, 2017), and that

this Ca^{2+}-dependent PLC isoform enhances osmotically evoked ΔN-TRPV1 currents that requires PKC activation (Bansal and Fisher, 2017).

1.5.3 Evidence for the role of PLCδ1 in modulating osmotically evoked F-actin polymerization and ΔN-TRPV1 currents

The findings by Bansal and Fisher in 2017 led our laboratory to hypothesize that the PLC isoform responsible could be a member of the PLCδ family (for more information on PLC mechanisms, see section 1.3.1.1). We sought to examine the role of the PLCδ1 isoform in osmoregulation by using transgenic mice that lacked this enzyme (PLCδ1 knockout [KO] mice). KO mice are genetically modified mice that have had their genomes altered to affect expression of certain proteins (Austin et al., 2004). We received PLCδ1 KO mice from colleagues in Japan (Yoshikazu Nakamura and Kiyoko Fukami). These KO mice lack PLCδ1 and do not express it anywhere in their bodies (Nakamura et al., 2003). Phenotypically, they do not appear to have an issue with drinking water or resting blood osmolality (Nakamura et al., 2003; Park et al., 2021). In our first experiment we subjected control (C57BL/6J) mice and PLCδ1 KO mice to 24-hour dehydration and examined their blood serum osmolality. The PLCδ1 KO mice exhibited significantly higher serum osmolality than the control mice, suggesting that their systemic osmoregulation is dysfunctional (Park et al., 2021). We next examined whether PLCδ1 played a role in F-actin polymerization. It was previously shown that Ang II-dependent F-actin polymerization in MNCs is activated by PLC (Zhang et al., 2007b; Prager-Khoutorsky and Bourque, 2010; Zhang and Bourque, 2008). We had also previously shown that osmotic PLC activation likely occurs in a manner similar to that of Ang II-mediated PLC activation and that the PLC isoform involved is

highly Ca^{2+}-dependent (Bansal and Fisher, 2017). We exposed isolated MNCs from control mice to hyperosmotic solution and found that hyperosmotic stimuli cause an increase in subcortical F-actin polymerization similar to that caused by Ang II (Park et al., 2021). However, when the same experiment was repeated in PLCδ1 KO mice, no osmotically induced increase in F-actin polymerization was observed (Park et al., 2021). Interestingly there was also no increase in F-actin in PLCδ1 KO mice when exposed to Ang II (Park et al., 2021). It is known that the PLC isoform involved in F-actin polymerization is from the PLCβ family (Poitras et al., 1998), but we suggested that PLCδ1 may be required for the full degree of F-actin polymerization and stimulation of PLCβ (Park et al., 2021). Next, we aimed to determine whether the MNCs of PLCδ1 produced osmotically evoked increases in MNC firing or ΔN-TRPV1 currents. We measured both parameters in control and PLCδ1 KO mice and observed an osmotically evoked increase in both AP firing and in ΔN-TRPV1 cation currents in control mice but not in PLCδ1 KO mice (Park et al., 2021). These findings led us to suggest that PLCδ1 plays a critical role in the osmotic activation of ΔN-TRPV1 and F-actin polymerization in MNCs (Park et al., 2021). The discovery of the potential involvement of PLCδ1 in MNC osmoregulation (Park et al., 2021) helps to further elucidate the physiological role of PLCδ1 in neurons as well as in potential underlying mechanisms of MNC osmoregulation.

1.6 Proposed model of osmosensory transduction in MNCs

Increases in external osmolality cause cellular shrinkage due to osmosis (refer to section 1.1 for more information on osmosis and cell volume changes). The cell shrinkage causes the mechanosensitive ΔN-TRPV1 channels present on the MNC plasma membrane to open (refer to

section 1.2.5 for more information on ΔN-TRPV1 channels), which then causes cation influx through ΔN-TRPV1 leading to MNC depolarization. This depolarization causes L-type Ca^{2+} channels present on the MNC plasma membrane to open and generate an influx of Ca^{2+}. In addition to the depolarization caused by ΔN-TRPV1, osmoreceptors from the OVLT and SFO increase their firing in response to the increase external osmolality and release GLUT onto MNCs, which then enables more cation influx and depolarization (refer to section 1.2.2 for more information on excitatory input from the OVLT and SFO onto MNCs). The high level of depolarization coming from ΔN-TRPV1 channels, L-type Ca^{2+} channels, and cation channels activated by GLUT stimulation enables MNCs to reach the depolarization threshold for AP firing and enhances MNC AP firing. The AP firing further enhances Ca^{2+} influx through L-type Ca^{2+} channels. The increase in $[Ca^{2+}]_i$ then activates a Ca^{2+}-dependent PLC isoform, which we believe to be PLCδ1 (based on the evidence presented in section 1.5.2 and section 1.5.3.). PLCδ1 then feeds back to ΔN-TRPV1 channels in a number of ways. PLCδ1 activation can enhance cortical F-actin polymerization, which enhances ΔN-TRPV1 mechanosensitivity and ability to transduce the hyperosmotically evoked decrease in cell volume into depolarizing currents. PLCδ1 also cleaves PIP_2 into IP_3 and DAG (refer to section 1.3.1.1 for more information on PLC), and the decrease in PIP_2 could modulate ΔN-TRPV1 activity (Lukacs et al., 2007). DAG then activates PKC, which can then phosphorylate ΔN-TRPV1 and enhance its activity (Bhave et al., 2002; Studer and McNaughton, 2010). These adaptations are all relatively rapid and can occur within minutes of exposure to hyperosmolality, and they could all contribute to the acute osmotic activation of MNCs, but we also propose a model for MNC adaptation to sustained exposure to hyperosmolality below.

CHAPTER 2: HYPOTHESES AND RESEARCH OBJECTIVES

Previous studies by our laboratory observed MNC hypertrophy *in vitro* and that it required APs, ΔN-TRPV1, PLC, PKC, Ca^{2+}, SNARE-mediated exocytosis and Ca^{2+} influx through L-type Ca^{2+} channels for hypertrophy to occur, and dynamin-mediated endocytosis for the recovery of hypertrophy to occur (Shah et al., 2014). We also observed that a Ca^{2+}-dependent isoform of PLC mediates osmotically evoked ΔN-TRPV1 currents (Bansal and Fisher, 2017). Our most recent study showed that PLCδ1 is involved in mediating osmotically evoked ΔN-TRPV1 currents and F-actin polymerization, and that mice that lack this enzyme exhibit dysfunctional systemic osmoregulation (Park et al., 2021). ΔN-TRPV1 is an important channel in osmoregulation (Zaelzer et al., 2015), produces increased currents during hyperosmotic challenge (Oliet and Bourque, 1993; Sharif-Naeini et al., 2006), and TRPV1 translocation occurs in other neurons and is mediated by PLC, PKC, and SNARE-mediated exocytosis (Morenilla-Palao et al., 2004; Planells-Cases et al., 2011; Camprubí-Robles et al., 2009). Based on these findings, our goal for this project was to determine whether an osmotically induced increase in the density of ΔN-TRPV1 channels on the MNC plasma membrane occurred and could contribute to how MNCs are able to sustain high AP firing and hormonal release under chronic osmotic stress.

We designed the following hypotheses and tested them using the *in vitro* model previously used by our laboratory to further study the possibility of osmotically induced ΔN-TRPV1 translocation in MNCs:

1. Hyperosmotic stimulation induces a reversible increase in MNC plasma membrane ΔN-TRPV1 density.
2. The osmotically induced increase in membrane ΔN-TRPV1 is PLC and PKC dependent.
3. The osmotically induced increase in membrane ΔN-TRPV1 requires SNARE-mediated exocytosis, and the recovery from the increase requires dynamin-mediated endocytosis.
4. The osmotically induced increase in membrane ΔN-TRPV1 requires translocation of vesicles from the Golgi to the plasma membrane.
5. The isoform of PLC responsible for the osmotic changes in plasma membrane ΔN-TRPV1 density is PLCδ1.

The objectives of this thesis are to elucidate the mechanisms surrounding sustained AP firing and hormone release, as well as hypertrophy, of MNCs exposed to high external osmolality. This project will aid in the understanding of the physiological relevance and function of osmotically evoked MNC hypertrophy, as well as to elucidate a possible mechanism by which MNCs are able to sustain a high degree of AP firing and hormone release during sustained exposure to hyperosmolality. These goals will enhance our understanding of the mechanisms underlying mammalian osmoregulation.

CHAPTER 3: MATERIALS AND METHODS

3.1 Ethical Approval

This work was approved by the University of Saskatchewan's Animal Research Ethics Board (Fisher: 2001-0066) and adhered to the Canadian Council on Animal Care guidelines for humane animal use.

3.2 Animals and Cellular Preparation

Male Long Evans rats aged 8-14 weeks were utilized for all rat experiments. Male C57BL/6J mice aged 8-10 weeks were utilized for the control mouse experiments. Both the rats and control mice were purchased from Charles River Laboratories (Laval, Quebec, Canada). PLCδ1 KO mice were originally acquired from Dr. Kiyoko Fukami of the Tokyo University of Pharmacy and Life Sciences in Japan, then bred in the University of Saskatchewan's Laboratory Animal Services Unit (LASU), then utilized at 8-10 weeks of age. All animals were anaesthetized using isoflurane and sacrificed by decapitation using a guillotine. Brains were promptly removed and tissue blocks containing a majority of the two supraoptic nuclei were immediately extracted from the brain and placed in an oxygenated (100% O_2) isotonic (295 ± 5 mOsm kg^{-1} for rats, 310 ± 5 mOsm kg^{-1} for mice) Pipes solution (pH 7.1) composed of (in mM): NaCl, 110; KCl, 5; $MgCl_2$, 1; $CaCl_2$, 1; Pipes, 20; glucose, 25, as well as bovine trypsin (Type XI, 0.6 mg mL^{-1}) in order to loosen the extracellular matrix surrounding the MNCs for 90 minutes at 37°C. Then, blocks were moved into an oxygenated isotonic PGC solution without trypsin and incubated for 30 minutes at room temperature (25℃; RT). Tissue blocks were then triturated using flame-polished pipettes until a

cell-suspension containing mostly isolated MNCs was reached (about 500 μL total volume). The cell-suspension solution was then plated evenly onto 3 glass-bottomed dishes and allowed to settle undisturbed for 20 minutes.

All drugs listed in section 3.3 were prepared in either water or dimethyl sulfoxide (DMSO). DMSO concentrations did not exceed 0.1% final volume, which has been proven to be safe for use in immunocytochemistry without toxic effects (Hanslick et al., 2009).

3.3 Drugs

3.3.1 U-73122

A non-selective competitive phospholipase C inhibitor (Smith et al., 1990). It was purchased from Enzo Life Sciences (Farmingdale, New York, USA) and applied to cells at a concentration of 1 μM, which was used previously by our laboratory (Shah et al., 2014).

3.3.2 Bisindolylmaleimide

A competitive broad-spectrum inhibitor of protein kinase C (Toullec et al., 1991). It was purchased from Sigma-Aldrich (St. Louis, Missouri, USA) and applied to cells at a concentration of 1 μM, which was used previously by our laboratory (Shah et al., 2014).

3.3.3 Dynasore

A competitive inhibitor of dynamin-mediated endocytosis (Macia et al., 2006). It was purchased from Sigma-Aldrich and applied to cells at a concentration of 80 μM, which was used previously by our laboratory (Shah et al., 2014).

3.3.4 Exo-1

A competitive inhibitor of exocytosis by inducing the collapse of the Golgi membrane(Feng et al., 2003). It was purchased from Selleck Chemicals (Houston, Texas, USA) and applied to cells at a concentration of 100 μM.

3.3.5 TAT-NSF700

A competitive inhibitor of SNARE-mediated exocytosis by blocking the function of N-ethylmaleimide-sensitive factor (NSF; Calvert et al., 2007). It was purchased from AnaSpec Inc. (Fremont, California, USA) and applied to cells at a concentration of 1.2 μM, which was used previously by our laboratory (Shah et al., 2014).

3.4 Live-cell ΔN-TRPV1 Immunocytochemistry

3.4.1 Isotonic, Hypertonic, Recovery

The 3 dishes were labeled: ISOTONIC (I), HYPERTONIC (H) and RECOVERY (R). Dishes were treated with 200 μL of either *isotonic* (295 $\pm$ 5 mOsm kg^{-1} for rats, 310 $\pm$ 5 mOsm kg $^{-1}$ for mice) or *hypertonic* (325 $\pm$ 5 mOsm kg^{-1} for rats, 340 $\pm$ 5 mOsm kg^{-1} for mice) oxygenated PGC and incubated for 15 minutes at RT. 200 μL of each solution was then removed from well and then 200 μL of either isotonic (I plate) or hypertonic (H and R plates) blocking solution (oxygenated Pipes + 5% donkey serum) was added to the corresponding wells and incubated for 45 minutes at RT. Next, 200 μL was removed from each well and 200 μL of isotonic (I and R plates) or hypertonic (H plate) primary antibody solution (oxygenated Pipes + 5% donkey serum + 3.3 μM anti-rat TRPV1 external epitope antibody [from Alomone Laboratories in Jerusalem, Isreal]) was added and incubated for 15 minutes at RT. It is important to note that the primary antibody is not cell-membrane permeable and would only bind to TRPV1 expressed on the plasma membrane. This antibody was affinity-purified by the manufacturer. 200 μL was then carefully removed from each well and dishes were then washed 3 times, 200 μL each time with either isotonic (I and R plates) or hypertonic (H plate) oxygenated 1x phosphate-buffered solution (PBS) to remove non-selective antibody binding. The 1x PBS was then removed from the wells and cells were fixated for 20 minutes at RT using 200 μL 4% paraformaldehyde (PFA) solution per dish. Once the PFA was removed plates were washed 3 times, 200 μL each time with 1x PBS + 0.1% Triton X-100 (PBST) in order to permeabilize the cells. It should be noted that permeabilization at this step is critical to allow the secondary antibody to penetrate the plasma membrane. After the PBST was

removed from the wells, 200 μL of secondary antibody solution (PGC + 5% donkey serum + 2 μM donkey anti-rabbit 488 nm light-sensitive secondary antibody [from Sigma-Aldrich in St. Louis, Missouri, USA]) was pipetted into the wells and the dishes were incubated in complete darkness for 1 hour at RT. After the secondary antibody solution was removed from each well, plates were washed 3 times, 200 μL each time with PBST, then once with 200 μL each 1x PBS in order to remove as much non-selective binding or excessive staining as possible. 200 μL of solution was removed from each well and Citifluor AF-1 antifade mounting solution (from Citifluor in Hatfield, Pennsylvania, USA) was added to each well. The I group was in isotonic solution for a total of 90 minutes before fixation. The H group was in hypertonic solution for a total of 90 minutes before fixation. The R group was in the hypertonic solution for 60 minutes, and the isotonic solution for 30 minutes before fixation. 60 minutes was sufficient time to cause significant hypertrophy and 30 minutes was sufficient enough to cause complete recovery. Treatment lengths were decided based on a previous paper (Shah et al., 2014) that used similar incubation times.

3.4.2 U-73122

3 dishes were labeled: ISOTONIC (I), HYPERTONIC (H), and U-73122 (U). A 100 μM stock solution of U-73122 in oxygenated hypertonic Pipes was used for all of the U treatments and diluted to 1 μM for each step (i.e., in the initial 15-minute treatment, the 45-minute blocking treatment, the 15-minute primary antibody treatment, and the 1x PBS washing) and then diluted to 1 μM for each step. The protocol for the I and H treatments identical to the one described in

isotonic, hypertonic, recovery. The U-73122 treatment was identical to the H treatment except for the presence of 1 μM of U-73122 in all steps prior to fixation.

3.4.3 Bisindolylmaleimide

3 dishes were labeled: ISOTONIC (I), HYPERTONIC (H), and BISINDOLYLMALEIMIDE (B). A 100 μM stock solution of bisindolylmaleimide in oxygenated hypertonic Pipes was used for all of the B treatments and diluted to 1 μM for each step (i.e., in the initial 15-minute treatment, the 45-minute blocking treatment, the 15-minute primary antibody treatment, and the 1x PBS washing). The protocol for the I and H treatments was identical to the one described in *isotonic, hypertonic, recovery*. The B treatment was identical to the H treatment except for the presence of 1 μM bisindolylmaleimide in all steps prior to fixation.

3.4.4 Dynasore

3 dishes were labeled: ISOTONIC (I), HYPERTONIC (H), and DYNASORE (D). A 1 mM stock solution of dynasore in oxygenated hypertonic Pipes was used for the initial 15-minute treatment and the 45-minute blocking treatment of the D plate. A 1 mM stock solution of dynasore in oxygenated isotonic Pipes was used for the 15-minute primary antibody treatment and the 1x PBS washing of the D plate. In each step the stock solution was diluted to 80 μM. The protocol for the I and H treatments was identical to the one described in *isotonic, hypertonic, recovery*. The D treatment was identical to the R treatment except for the presence of 80 μM dynasore in all steps prior to fixation.

3.4.5 Exo-1

3 dishes were labeled: ISOTONIC (I), HYPERTONIC (H), and EXO-1 (E). A 1 mM stock solution of Exo-1 in oxygenated hypertonic Pipes was used for all of the E treatments and diluted to 100 μM for each step (i.e., in the initial 15-minute treatment, the 45-minute blocking treatment, the 15-minute primary antibody treatment, and the 1x PBS washing). The protocol for the I and H treatments was identical to the one described in *isotonic, hypertonic, recovery*. The E treatment was identical to the H treatment except for the presence of 100 μM Exo-1 in all steps prior to fixation.

3.4.6 TAT-NSF700

3 dishes were labeled: ISOTONIC (I), HYPERTONIC (H), and TAT-NSF700 (T). A 100 μM stock solution of bisindolylmaleimide in oxygenated hypertonic Pipes was used for all of the T treatments and diluted to 1.2 μM for each step (i.e., in the initial 15-minute treatment, the 45-minute blocking treatment, the 15-minute primary antibody treatment, and the 1x PBS washing). The protocol for the I and H treatments was identical to the one described in *isotonic, hypertonic, recovery*. The T treatment was identical to the H treatment except for the presence of 1.2 μM TAT-NSF700 in all steps prior to fixation.

CHAPTER 4: DATA COLLECTION AND STATISTICAL ANALYSIS

Images were captured using a Carl Zeiss LSM700 Laser Scanning Microscope (Jena, Germany) using a 40x oil-immersion objective. Plates were scanned under the fluorescence of a 470 nm laser as this was close to the excitation wavelength of the fluorescent tag AlexaFluor 488 attached to the secondary antibody (excitation λ = 495 nm; emission λ = 519 nm). The Carl Zeiss Zen Black software was used for image capturing on all experiments. Digital gain voltage and laser intensity were optimized for the primary experiment to establish a baseline of immunofluorescence that was neither over- or under-exposed according to Zen Black, and parameters were thereafter kept constant for all experiments to maintain consistency. Any cell that appeared to have a defined membrane, an oval-type shape typical of MNCs, and at least one foot process (i.e., somatic dendrite) extending from the cell body was deemed healthy and captured for further analysis. Cells that appeared lysed, circular, or without a foot process were deemed unhealthy and were not captured, as the goal of the experiment was to examine healthy MNCs. The criteria above for identifying a healthy MNC was based off of a previous study (Oliet and Bourque, 1992). This group also established a criterion for MNC cell size, where 97% of cells with a cross-sectional area (CSA) $\geq$ 200 μm^2 were deemed MNCs in rats (Oliet and Bourque, 1992) and in control mice (Sharif-Naeini et al., 2008). Z-stack images were captured for all images in order to examine captured cells from multiple stage depths. Images were saved periodically as both the original Zeiss (.czi) as well as a high-resolution file (.TIFF) compatible with the software utilized for analysis. All image analysis was performed using the software ImageJ (from the National Institute of Health [NIH] in Bethesda, Maryland, USA). This software had previously been used for MNC analysis in our laboratory (Shah et al., 2014; Bansal and Fisher, 2017; Park et al., 2021). A 2 μm^2-wide pixel brush tool was used to trace the membrane of captured cells. Foot processes were not

included in the trace as our focus was plasma membrane ΔN-TRPV1 density on the cell body. Cells chosen to be analyzed were chosen by the definition of the cell membrane and foot process (i.e., cell shape and appearance). Microsoft Excel was used to compile the data into charts, and GraphPad Prism 7 was used for statistical analysis and graphical production. The cell body membrane immunofluorescence and cross-sectional area (CSA) from cells in each treatment group were collected in Excel each day analysis was performed. The mean values for each treatment group's immunofluorescence and CSA were then calculated and stored in a master Excel file containing the mean values of all treatment groups from each day of experimentation and grouped as data sets. All 'n' values therefore represent of the number of animals used, not the number of cells analyzed. In order for a plate to be considered usable in the data set, at least 8 cells from the plate had to be deemed healthy MNCs by the criteria established above. All plates that were imaged had between 8-20 usable cells. Every cell that appeared healthy under the microscope was captured and analyzed using ImageJ. Since isotonic and hypertonic treatment groups were performed alongside each other experimental treatment, the n value of the isotonic and hypertonic groups in rats was significantly higher than the other treatments (n= 53 total experiments for isotonic and hypertonic treatments compared to n= 8-11 for each other experimental treatment) the data sets were split by experiment. For example, the isotonic and hypertonic treatments that were performed with the recovery, U-731212, and bisindolylmaleimide experiments were grouped together (as seen in Figure 5.2A), and the isotonic and hypertonic treatments that were performed alongside the dynasore, Exo-1, and TAT-NSF700 experiments were grouped together (as seen in Figure 5.2B). All control and PLCδ1 KO mouse data sets were grouped as one because fewer total experiments were performed (as seen in Figure 5.4 and Figure 5.8, respectively). One-way analysis-of-variance (ANOVA) with Bonferroni's post-hoc test was performed on each data set in

order to get a comparison of the means of the data between experimental groups. All data are expressed as the mean $\pm$ standard deviation (SD). Results were deemed statistically significant if $P < 0.05$ (*), $P < 0.01$ (**), and $P < 0.001$ (***). Results for ΔN-TRPV1 immunofluorescence are expressed in arbitrary units (a.u.) and results for CSA are expressed in μm^2.

CHAPTER 5: RESULTS

5.1 Osmotically induced changes in MNC plasma membrane ΔN-TRPV1 immunofluorescence under different experimental conditions

The goal of these experiments was to test the hypothesis that hyperosmotic stimulation of isolated MNCs triggers ΔN-TRPV1 translocation, and to examine the parameters required for this translocation to occur.

5.1.1 Hyperosmotic stimulation induces a reversible increase in plasma membrane ΔN-TRPV1 levels

MNC plasma membrane ΔN-TRPV1 immunofluorescence was examined in isotonic, hypertonic, and recovery treatments (refer to section 3.4.1). MNCs placed in a hypertonic solution displayed a significant increase in ΔN-TRPV1 immunofluorescence compared to MNCs in an isotonic solution in rats (isotonic: 21.54 ± 2.387, n= 29 to hypertonic: 29.32 ± 2.894, n= 29, P< 0.001) and in control mice (isotonic: 22.30 ± 1.146, n= 16 to hypertonic: 30.40 ± 1.797, n= 16, P < 0.001). MNCs in the recovery treatment displayed ΔN-TRPV1 immunofluorescence that was significantly lower than the hypertonic treatment in rats (hypertonic: 29.32 ± 2.894, n= 29 to recovery: 22.67 ± 2.894, n=11, P < 0.001) and in control mice (hypertonic: 30.40 ± 1.797, n= 16 to recovery: 23.86 ± 0.939, n= 8, P < 0.001). There was no significant difference between the isotonic and recovery groups in rats (isotonic: 21.54 ± 2.387, n= 29 to recovery: 22.67 ± 2.894, n=11, ns) and in control mice (isotonic: 22.30 ± 1.146, n= 16 to recovery: 23.86 ± 0.939, n= 8, ns). These data

suggest that there is an osmotically induced increase of plasma membrane ΔN-TRPV1 that occurs in MNCs and that this process is reversible in both rats and control mice.

5.1.2 Osmotically induced increases in plasma membrane ΔN-TRPV1 are PLC-dependent

MNCs placed in a hypertonic solution containing 1 μM U-73122 (refer to section 3.4.2) exhibited significantly lower ΔN-TRPV1 immunofluorescence compared to MNCs placed in a hypertonic solution without U-73122 in rats (hypertonic: 29.32 $\pm$ 2.894, n= 29 to U-73122: 20.87 $\pm$ 1.105, n= 10, $P < 0.001$). There was no significant difference between the isotonic and U-73122 treatment groups in rats (isotonic: 21.54 $\pm$ 2.387, n= 29 to U-73122: 20.87 $\pm$ 1.105, n= 10, ns). These data suggest that the inhibition of PLC by U-73122 prevents osmotically induced increases in plasma membrane ΔN-TRPV1.

5.1.3 Osmotically induced increases in plasma membrane ΔN-TRPV1 are PKC-dependent

MNCs placed in a hypertonic solution containing 1 μM bisindolylmaleimide (refer to section 3.4.3) exhibited significantly lower ΔN-TRPV1 immunofluorescence compared to MNCs placed in a hypertonic solution without bisindolylmaleimide in rats (hypertonic: 29.32 $\pm$ 2.894, n= 29 to bisindolylmaleimide: 21.51 $\pm$ 1.050, n= 8, $P < 0.001$). There was no significant difference between the isotonic and bisindolylmaleimide treatment groups in rats (isotonic: 21.54 $\pm$ 2.387, n= 29 to bisindolylmaleimide: 21.51 $\pm$ 1.050, n= 8, ns). These data suggest that the inhibition of PKC by bisindolylmaleimide prevents osmotically induced increases in plasma membrane ΔN-TRPV1.

5.1.4 Endocytosis is required for the reversal of osmotically induced increases in plasma membrane ΔN-TRPV1

MNCs placed in a hypertonic solution, then an isotonic solution, both of which containing 80 μM dynasore (refer to section 3.4.4) exhibited a significantly higher plasma membrane ΔN-TRPV1 immunofluorescence compared to the isotonic treatment in rats (isotonic: 22.65 $\pm$ 1.099, n= 24 to dynasore: 31.56 $\pm$ 1.652, n= 8, $P < 0.001$). There was also a significant difference between the recovery and dynasore treatments in rats (recovery: 22.67 $\pm$ 2.894, n=11 to dynasore: 31.56 $\pm$ 1.652, n= 8, $P < 0.001$). There was no significant difference between the hypertonic and dynasore treatments in rats (hypertonic: 30.45 $\pm$ 1.274, n= 24 to dynasore: 31.56 $\pm$ 1.652, n= 8, ns). Because there was a significant difference between the recovery and dynasore treatments and the protocols were identical except for the presence of 80 μM dynasore, the data suggests that endocytosis is required for the reversal of the osmotically induced increase in plasma membrane ΔN-TRPV1.

5.1.5 Osmotically induced increases in plasma membrane ΔN-TRPV1 require Golgi-derived vesicles

MNCs placed in a hypertonic solution containing 100 μM Exo-1 (refer to section 3.4.5) exhibited significantly lower ΔN-TRPV1 immunofluorescence compared to MNCs placed in a hypertonic solution without Exo-1 in rats (hypertonic: 30.45 $\pm$ 1.274, n= 24 to Exo-1: 21.49 $\pm$ 0.8827, n= 8, $P < 0.001$) and in control mice (hypertonic: 30.40 $\pm$ 1.797, n= 16 to Exo-1: 22.41 $\pm$ 0.9389, n= 8, $P < 0.001$). There was no significant difference between the isotonic and Exo-1 treatment groups in rats (isotonic: 22.65 $\pm$ 1.099, n= 24 to Exo-1: 21.49 $\pm$ 0.8827, n= 8, ns) and in control mice

(isotonic: 22.30 ± 1.146, n= 16 to Exo-1: 22.41 ± 0.5891, n= 8, ns). These data suggest that the inhibition of exocytosis by Exo-1 prevents osmotically induced increases in plasma membrane ΔN-TRPV1.

5.1.6 Osmotically induced increases in plasma membrane ΔN-TRPV1 require SNARE-mediated exocytosis

MNCs placed in a hypertonic solution containing 1.2 μM TAT-NSF700 (refer to section 3.4.6) exhibited significantly lower ΔN-TRPV1 immunofluorescence compared to MNCs placed in a hypertonic solution without TAT-NSF700 in rats (hypertonic: 30.45 ± 1.274, n= 24 to TAT-NSF700: 21.86 ± 1.019, n= 8, $P < 0.001$). There was no significant difference between the isotonic and TAT-NSF700 treatment groups in rats (isotonic: 22.65 ± 1.099, n= 24 to TAT-NSF700: 21.86 ± 1.019, n= 8, ns). These data suggest that the inhibition of SNARE-mediated exocytotic membrane fusion by TAT-NSF700 prevents osmotically induced increases in plasma membrane ΔN-TRPV1.

The results from the experiments conducted in this section suggest that reversible osmotically induced ΔN-TRPV1 translocation occurs in MNCs, and that PLC, PKC, Golgi-derived vesicles, and SNARE-mediated exocytosis are required for the translocation, and that dynamin-mediated endocytosis is required for the internalization of ΔN-TRPV1 from the plasma membrane.

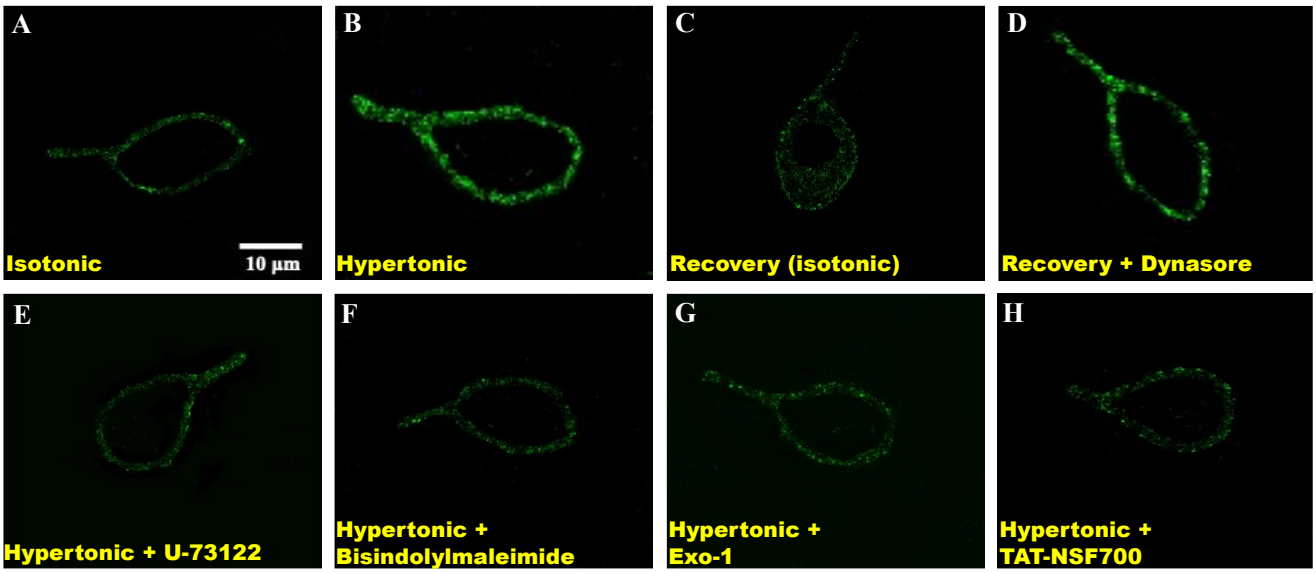

Figure 5.1: Immunocytochemistry images depicting osmotically induced changes in rat MNC plasma membrane ΔN-TRPV1 immunofluorescence under different experimental conditions. Representative immunocytochemistry images of the graphs presented in Figure 5.2 and Figure 5.5. (A) Isotonic treatment (295 ± 5 mosmol kg^{-1}). (B) Hypertonic treatment (325 ± 5 mosmol kg^{-1}). (C) Recovery treatment (hypertonic, then isotonic). (D) Recovery treatment + 80 μM dynasore. (E) Hypertonic treatment + 1 μM U-73122. (F) Hypertonic treatment + 1 μM bisindolylmaleimide. (G) Hypertonic treatment + 100 μM Exo-1. (H) Hypertonic treatment + 1.2 μM TAT-NSF700.

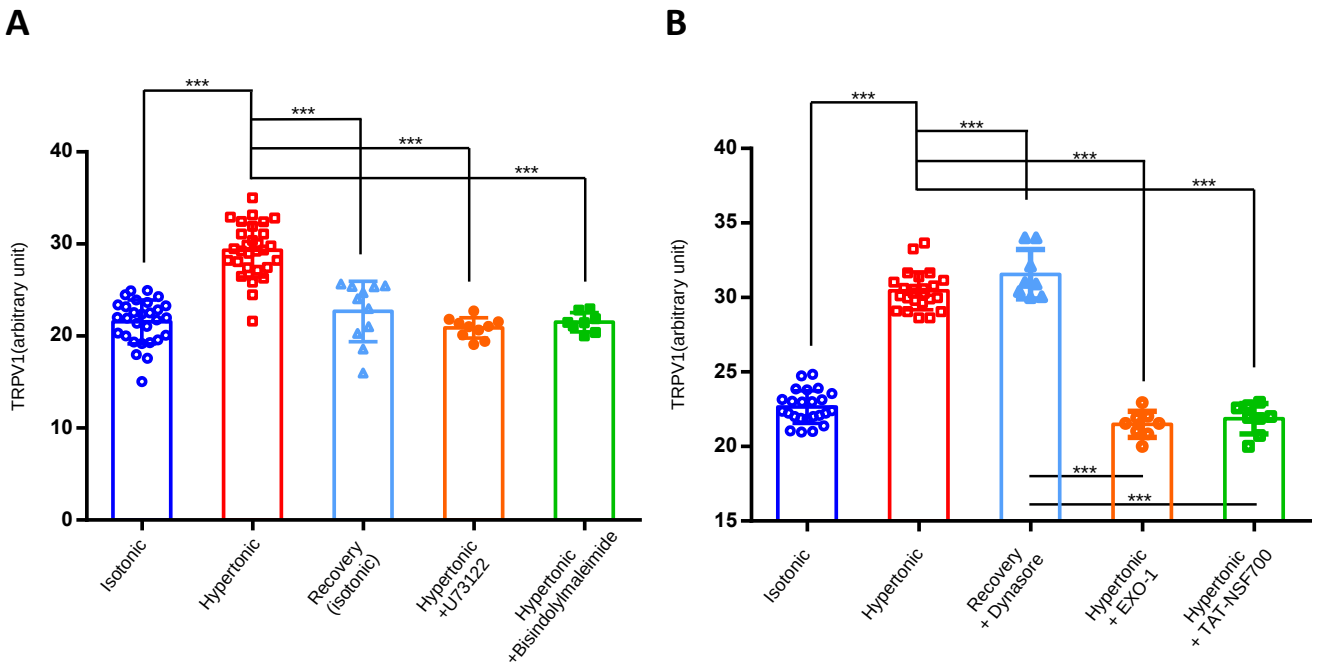

Figure 5.2: Osmotically induced changes in rat MNC plasma membrane ΔN-TRPV1 immunofluorescence under different experimental conditions. (A) Bar-scatter plot showing that osmotically induced increases in plasma membrane TRPV1 immunofluorescence occur, are reversible, and require activation of PLC and PKC. TRPV1 labeling of isolated MNCs in hypertonic solution was significantly higher than in isotonic solution (isotonic: 21.54 ± 2.387, n= 29 to hypertonic: 29.32 ± 2.894, n= 29, P< 0.001). TRPV1 labeling was significantly reduced with a washout of hypertonic solution with isotonic solution in the recovery treatment (hypertonic: 29.32 ± 2.894, n= 29 to recovery: 22.67 ± 2.894, n=11, P < 0.001), as well as by the presence of the PLC inhibitor U-73122 (hypertonic: 29.32 ± 2.894, n= 29 to U-73122: 20.87 ± 1.105, n= 10, P < 0.001) and by the PKC inhibitor bisindolylmaleimide (hypertonic: 29.32 ± 2.894, n= 29 to bisindolylmaleimide: 21.51 ± 1.050, n= 8, P < 0.001). (B) Bar-scatter plot showing that the retrieval of TRPV1 from the plasma membrane requires dynamin-mediated endocytosis, and that

osmotically induced increases in plasma membrane TRPV1 immunofluorescence require vesicles from the Golgi and SNARE-mediated exocytosis. TRPV1 labeling of isolated MNCs in recovery solution (hypertonic with isotonic washout) containing the dynamin inhibitor dynasore was significantly higher than the isotonic treatment (isotonic: 22.65 $\pm$ 1.099, n= 24 to dynasore: 31.56 $\pm$ 1.652, n= 8, $P < 0.001$). TRPV1 labeling was significantly diminished in isolated MNCs in hypertonic solution containing the Golgi inhibitor Exo-1 (hypertonic: 30.45 $\pm$ 1.274, n= 24 to Exo-1: 21.49 $\pm$ 0.8827, n= 8, $P < 0.001$) or an inhibitor of SNARE-mediated exocytosis, TAT-NSF700 (hypertonic: 30.45 $\pm$ 1.274, n= 24 to TAT-NSF700: 21.86 $\pm$ 1.019, n= 8, $P < 0.001$). For (A), $F(4, 87) = 37.52$. For (B), $F(4, 67) = 223.3$.

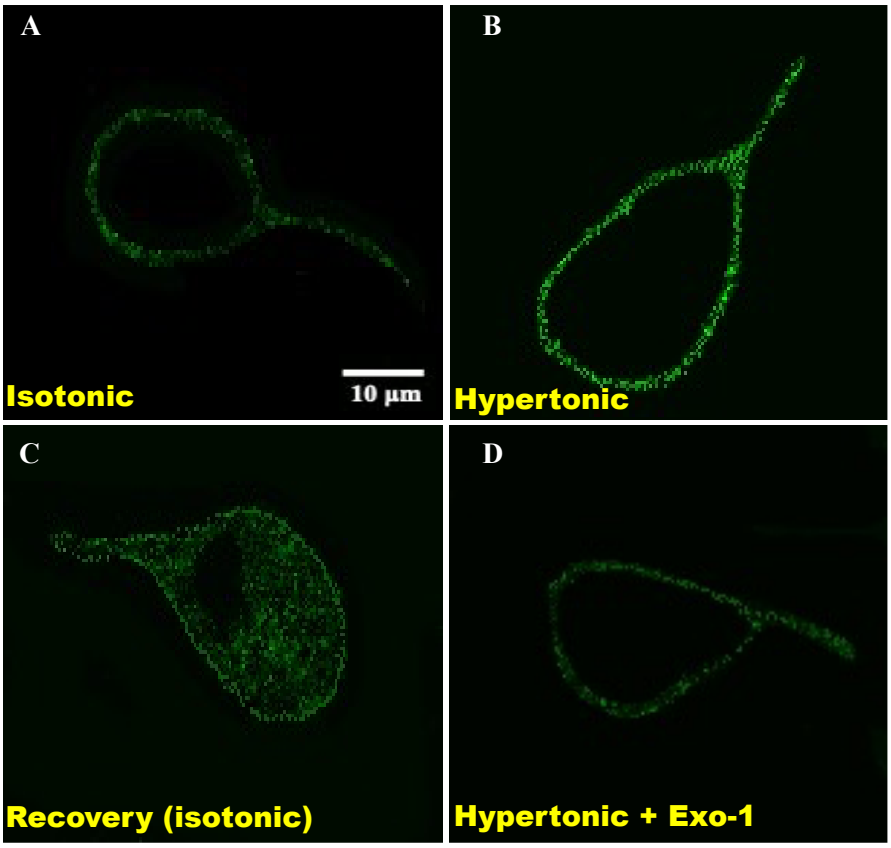

Figure 5.3: Immunocytochemistry images depicting osmotically induced changes in C57BL/6J (control) mouse MNC plasma membrane ΔN-TRPV1 immunofluorescence under different experimental conditions. Representative immunocytochemistry images of the graphs presented in Figure 5.4 and Figure 5.6. (A) Isotonic treatment (310 ± 5 mosmol kg^{-1}). (B) Hypertonic treatment (340 ± 5 mosmol kg^{-1}). (C) Recovery treatment (hypertonic, then isotonic). (D) Hypertonic treatment + 100 μM Exo-1.

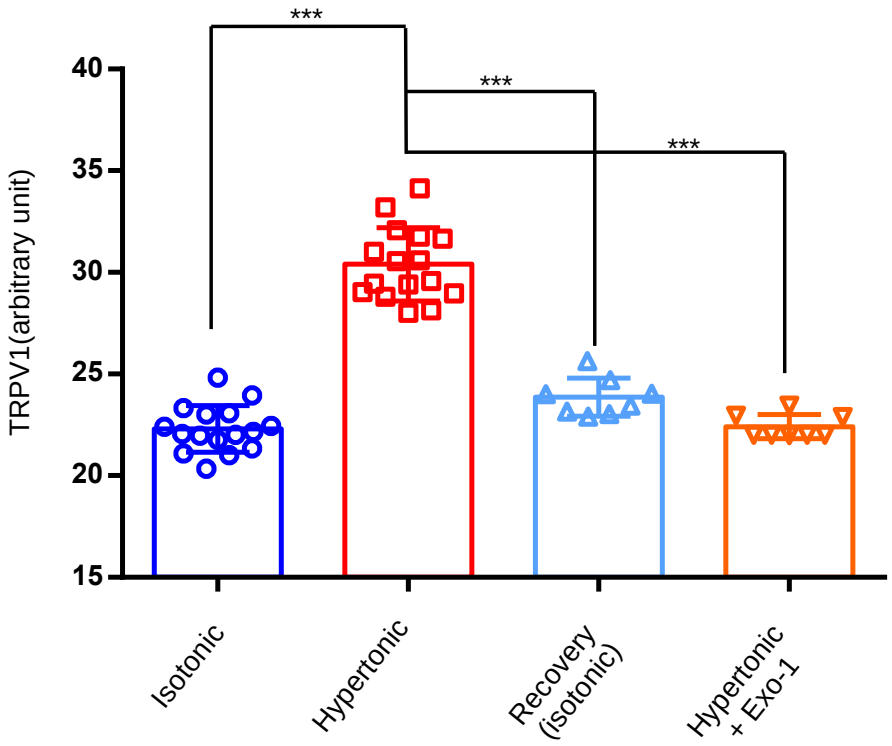

Figure 5.4: Osmotically induced changes in C57BL/6J (control) mouse MNC plasma membrane ΔN-TRPV1 immunofluorescence under different experimental conditions. Bar-scatter plot showing that osmotically induced increases in plasma membrane TRPV1 immunofluorescence occur, are reversible, and require vesicles from the Golgi. TRPV1 labeling of isolated MNCs in hypertonic solution was significantly higher than in isotonic solution (isotonic: 22.30 ± 1.146, n= 16 to hypertonic: 30.40 ± 1.797, n= 16, $P < 0.001$). TRPV1 labeling was significantly reduced with a washout of hypertonic solution with isotonic solution in the recovery treatment (hypertonic: 30.40 ± 1.797, n= 16 to recovery: 23.86 ± 0.939, n= 8, $P < 0.001$), or by the presence of the Golgi inhibitor Exo-1 (hypertonic: 30.40 ± 1.797, n= 16 to Exo-1: 22.41 ± 0.9389, n= 8, $P < 0.001$). $F(3, 44) = 122.9$.

5.2 Osmotically induced changes in MNC cross-sectional area under different experimental conditions

The experiments conducted previously by our laboratory (Shah et al., 2014) showed that MNC hypertrophy requires PLC, PKC, and SNARE-mediated exocytosis, and that the recovery from hypertrophy requires dynamin-mediated endocytosis. These experiments were repeated to examine whether there are commonalities in the mechanisms governing osmotically evoked MNC hypertrophy and osmotically induced ΔN-TRPV1 translocation. They were then conducted in control mice to observe whether the model was valid in mice.

5.2.1 Reversible osmotically induced increases in MNC cross-sectional area (CSA)

MNC CSA was examined in isotonic, hypertonic, and recovery treatments (refer to section 3.4.1). MNCs placed in a hypertonic solution displayed a significant increase CSA compared to MNCs in an isotonic solution in rats (isotonic: 319.97 $\pm$ 9.1740 μm^2, n= 29 to hypertonic: 347.05 $\pm$ 15.325 μm^2, n= 29, P< 0.001) and in control mice (isotonic: 237.71 $\pm$ 3.3900 μm^2, n= 16 to hypertonic: 266.91 $\pm$ 7.8319 μm^2, n= 16, P < 0.001). MNCs in the recovery treatment exhibited significantly lower CSA than the hypertonic treatment in rats (hypertonic: 347.05 $\pm$ 15.325 μm^2, n= 29 to recovery: 336.92 $\pm$ 12.730 μm^2, n=11, P < 0.001) and in control mice (hypertonic: 266.91 $\pm$ 7.8319 μm^2, n= 16 to recovery: 246.46 $\pm$ 2.8070 μm^2, n= 8, P < 0.001). There was no significant difference between the isotonic and recovery groups in rats (isotonic: 319.97 $\pm$ 9.1740 μm^2, n= 29 to recovery: 336.92 $\pm$ 12.730 μm^2, n=11, ns) and in control mice (isotonic: 237.71 $\pm$ 3.3900 μm^2,

n= 16 to recovery: 246.46 ± 2.8070 μm^2, n= 8, ns). These data suggest that there is an osmotically induced increase of MNC CSA that occurs and is reversible in both rats and control mice.

5.2.2 Osmotically induced increases in MNC CSA are PLC-dependent

MNCs placed in a hypertonic solution containing 1 μM U-73122 (refer to section 3.4.2) exhibited significantly lower CSA compared to MNCs placed in a hypertonic solution without U-73122 in rats (hypertonic: 347.05 ± 15.325 μm^2, n= 29 to U-73122: 314.93 ± 9.1992 μm^2, n= 10, $P < 0.001$). There was no significant difference between the isotonic and U-73122 treatment groups in rats (isotonic: 319.97 ± 9.1740 μm^2, n= 29 to U-73122: 314.93 ± 9.1992 μm^2, n= 10, ns). These data suggest that the inhibition of PLC by U-73122 prevents osmotically induced increases in MNC CSA from occurring.

5.2.3 Osmotically induced increases in MNC CSA are PKC-dependent

MNCs placed in a hypertonic solution containing 1 μM bisindolylmaleimide (refer to section 3.4.3) exhibited significantly lower CSA compared to MNCs placed in a hypertonic solution without bisindolylmaleimide in rats (hypertonic: 347.05 ± 15.325 μm^2, n= 29 to bisindolylmaleimide: 320.28 ± 3.2160 μm^2, n= 8, $P < 0.001$). There was no significant difference between the isotonic and bisindolylmaleimide treatment groups in rats (isotonic: 319.97 ± 9.1740 μm^2, n= 29 to bisindolylmaleimide: 320.28 ± 3.2160 μm^2, n= 8, ns). These data suggest that the inhibition of PKC by bisindolylmaleimide prevents osmotically induced increases in MNC CSA from occurring.

5.2.4 Endocytosis is required for the reversal of osmotically induced increases in MNC CSA

MNCs placed in a hypertonic solution, then an isotonic solution, both of which containing 80 μM dynasore (refer to section 3.4.4) exhibited a significant increase in CSA compared to the isotonic treatment in rats (isotonic: 322.396 $\pm$ 4.413 μm^2, n= 24 to dynasore: 352.51 $\pm$ 5.8086 μm^2, n= 8, $P < 0.001$). There was also a significant difference between the recovery and dynasore treatments in rats (recovery: 336.92 $\pm$ 12.730 μm^2, n=11 to dynasore: 352.51 $\pm$ 5.8086 μm^2, n= 8, $P < 0.001$). There was no significant difference between the hypertonic and dynasore treatments in rats (hypertonic: 339.31 $\pm$ 7.9328 μm^2, n= 24 to dynasore: 352.51 $\pm$ 5.8086 μm^2, n= 8, ns). Because there was a significant difference between the recovery and dynasore treatments and the protocols were identical except for the presence of 80 μM dynasore in the dynasore treatment, the data suggests that endocytosis is required for the reversal of the osmotically induced increase in MNC CSA.

5.2.5 Osmotically induced increases in MNC CSA require Golgi-derived vesicles

MNCs placed in a hypertonic solution containing 100 μM Exo-1 (refer to section 3.4.5) exhibited significantly lower CSA compared to MNCs placed in a hypertonic solution without Exo-1 in rats (hypertonic: 339.31 $\pm$ 7.9328 μm^2, n= 24 to Exo-1: 315.80 $\pm$ 2.2635 μm^2, n= 8, $P < 0.001$) and in control mice (hypertonic: 266.91 $\pm$ 7.8320 μm^2, n= 16 to Exo-1: 235.25 $\pm$ 3.9890 μm^2, n= 8, $P < 0.001$). There was no significant difference between the isotonic and Exo-1 treatment groups in rats (isotonic: 322.396 $\pm$ 4.413 μm^2, n= 24 to Exo-1: 315.80 $\pm$ 2.2635 μm^2, n= 8, ns) and in control mice (isotonic: 237.71 $\pm$ 3.3900 μm^2, n= 16 to Exo-1: 315.80 $\pm$ 2.2635 μm^2, n= 8, ns). These data

suggest that the inhibition of exocytosis by Exo-1 prevents osmotically induced increases in MNC CSA from occurring.

5.2.6 Osmotically induced increases in MNC CSA require SNARE-mediated exocytosis

MNCs placed in a hypertonic solution containing 1.2 μM TAT-NSF700 (refer to section 3.4.6) exhibited significantly lower CSA compared to MNCs placed in a hypertonic solution without TAT-NSF700 in rats (hypertonic: 339.31 $\pm$ 7.9328 μm^2, n= 24 to TAT-NSF700: 317.224 $\pm$ 3.0330 μm^2, n= 8, $P < 0.001$). There was no significant difference between the isotonic and TAT-NSF700 treatment groups in rats (isotonic: 322.396 $\pm$ 4.413 μm^2, n= 24 to TAT-NSF700: 317.224 $\pm$ 3.0330 μm^2, n= 8, ns). These data suggest that the inhibition of SNARE-mediated exocytotic membrane fusion by TAT-NSF700 prevents osmotically induced increases in MNC CSA from occurring.

These data confirm that osmotically evoked MNC hypertrophy occurs in control mice, and that there are commonalities in the mechanisms governing osmotically induced ΔN-TRPV1 translocation and hypertrophy.

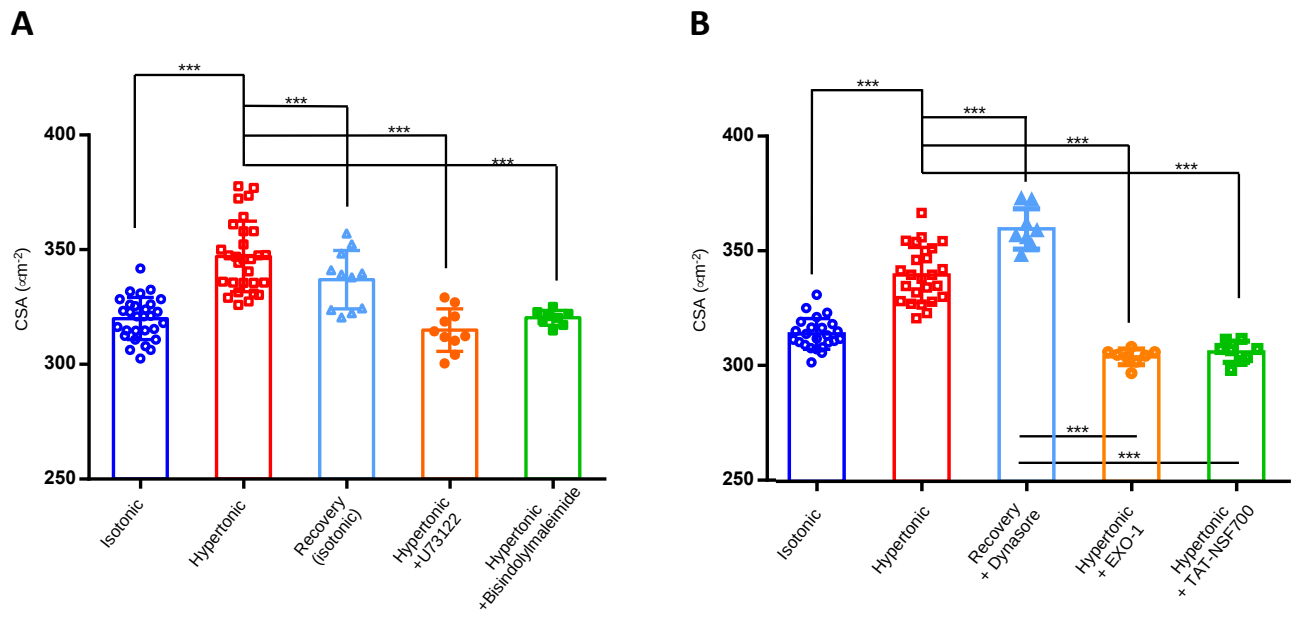

Figure 5.5: Osmotically induced changes in rat MNC cross-sectional area (CSA) under different experimental conditions. (A) Bar-scatter plot showing that osmotically induced increases in MNC CSA occur, are reversible, and require activation of PLC and PKC. CSA of isolated MNCs in hypertonic solution was significantly higher than in isotonic solution (isotonic: 319.97 ± 9.1740 μm^2, n= 29 to hypertonic: 347.05 ± 15.325 μm^2, n= 29, P< 0.001). CSA was significantly reduced with a washout of hypertonic solution with isotonic solution in the recovery treatment (hypertonic: 347.05 ± 15.325 μm^2, n= 29 to recovery: 336.92 ± 12.730 μm^2, n=11, P < 0.001), as well as by the presence of the PLC inhibitor U-73122 (hypertonic: 347.05 ± 15.325 μm^2, n= 29 to U-73122: 314.93 ± 9.1992 μm^2, n= 10, P < 0.001) and by the PKC inhibitor bisindolylmaleimide (hypertonic: 347.05 ± 15.325 μm^2, n= 29 to bisindolylmaleimide: 320.28 ± 3.2160 μm^2, n= 8, P < 0.001). (B) Bar-scatter plot showing that dynamin-mediated endocytosis is required for the recovery from hypertrophy, and that osmotically induced increases in MNC CSA require vesicles from the Golgi and SNARE-mediated exocytosis. TRPV1 labeling of isolated

MNCs in recovery solution (hypertonic with isotonic washout) containing the dynamin inhibitor dynasore was significantly higher than the isotonic treatment (isotonic: 322.396 $\pm$ 4.413 μm^2, n= 24 to dynasore: 352.51 $\pm$ 5.8086 μm^2, n= 8, $P < 0.001$). TRPV1 labeling was significantly diminished in isolated MNCs in hypertonic solution containing the Golgi inhibitor Exo-1 (hypertonic: 339.31 $\pm$ 7.9328 μm^2, n= 24 to Exo-1: 315.80 $\pm$ 2.2635 μm^2, n= 8, $P < 0.001$) or an inhibitor of SNARE-mediated exocytosis, TAT-NSF700 (hypertonic: 339.31 $\pm$ 7.9328 μm^2, n= 24 to TAT-NSF700: 317.224 $\pm$ 3.0330 μm^2, n= 8, $P < 0.001$). For (A), $F(5, 87) = 23.62$. For (B), $F(4, 67) = 78.36$.

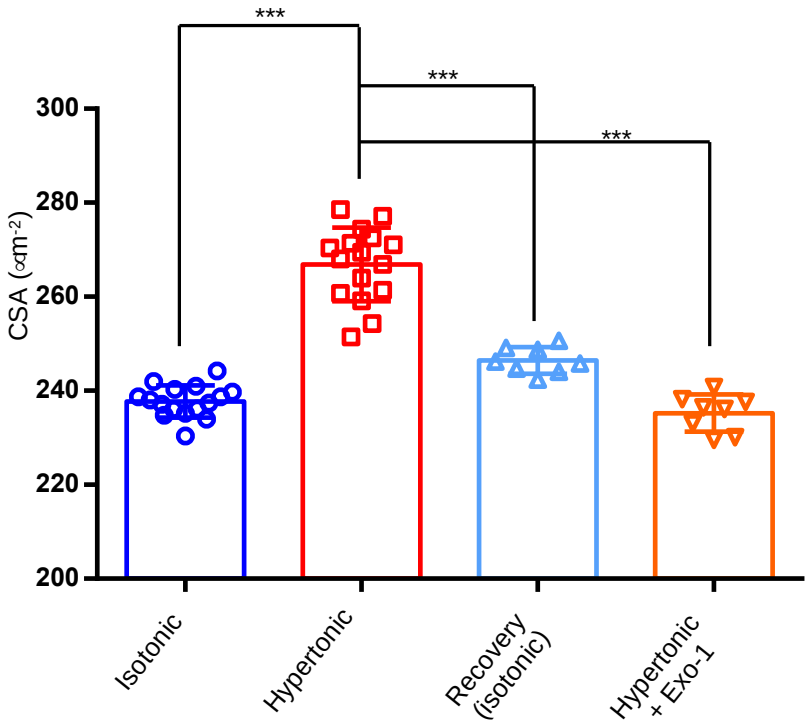

Figure 5.6: Osmotically induced changes in C57BL/6J (control) mouse MNC cross-sectional area (CSA) under different experimental conditions. Bar-scatter plot showing that osmotically induced increases in MNC CSA occur, are reversible, and require vesicles from the Golgi. CSA of isolated MNCs in hypertonic solution was significantly higher than in isotonic solution (isotonic: 237.71 ± 3.3900 μm^2, n= 16 to hypertonic: 266.91 ± 7.8319 μm^2, n= 16, $P < 0.001$). CSA was significantly reduced with a washout of hypertonic solution with isotonic solution in the recovery treatment (hypertonic: 266.91 ± 7.8319 μm^2, n= 16 to recovery: 246.46 ± 2.8070 μm^2, n= 8, $P < 0.001$), or by the presence of the Golgi inhibitor Exo-1 (hypertonic: 266.91 ± 7.8320 μm^2, n= 16 to Exo-1: 235.25 ± 3.9890 μm^2, n= 8, $P < 0.001$). $F(3, 44) = 101.6$.

5.3 PLCδ1 KO mouse MNCs display impaired responses to hyperosmolality

After confirming that osmotically induced ΔN-TRPV1 translocation and osmotically evoked MNC hypertrophy occur in both rats and mice, and that both require PLC, our next test was to repeat the experiments in PLCδ1 KO mice to determine whether PLCδ1 is required for ΔN-TRPV1 translocation and hypertrophy.

5.3.1 Osmotically induced increases in plasma membrane ΔN-TRPV1 require PLCδ1

The experiment described in section 3.4.1 was repeated in PLCδ1 KO mice. MNCs placed in a hypertonic solution did not display a difference in ΔN-TRPV1 immunofluorescence compared to MNCs in an isotonic solution (isotonic: 21.37 $\pm$ 0.5200, n= 8 to hypertonic: 21.31 $\pm$ 0.4385, n= 8, ns). MNCs in the recovery treatment also did not display any difference in ΔN-TRPV1 immunofluorescence compared to either the isotonic treatment (isotonic: 21.37 $\pm$ 0.5200, n= 8 to recovery: 21.15 $\pm$ 0.3823, n= 8, ns) or the hypertonic treatment (hypertonic: 21.31 $\pm$ 0.4385, n= 8 to recovery: 21.15 $\pm$ 0.3823, n= 8, ns). These data suggest that PLCδ1 is required for the osmotically induced increase in ΔN-TRPV1 immunofluorescence, as the increase observed in both rats and in control mice is not observed in PLCδ1 KO mice.

5.3.2 Osmotically induced increases in MNC CSA require PLCδ1

The experiment described section 3.4.1 was repeated in PLCδ1 KO mice. MNCs placed in a hypertonic solution did not display a difference in CSA compared to MNCs in an isotonic solution

(isotonic: 233.10 ± 2.1726 μm^2, n= 8 to hypertonic: 233.11 ± 1.7395 μm^2, n= 8, ns). MNCs in the recovery treatment also did not display any difference in ΔN-TRPV1 immunofluorescence compared to either the isotonic treatment (isotonic: 233.10 ± 2.1726 μm^2, n= 8 to recovery: 232.50 ± 1.6393 μm^2, n= 8, ns) or the hypertonic treatment (hypertonic: 233.11 ± 1.7395 μm^2, n= 8 to recovery: 232.50 ± 1.6393 μm^2, n= 8, ns). These data suggest that PLCδ1 is also required for the osmotically induced increase in MNC CSA, as the increase observed in both rats and in control mice is not observed in PLCδ1 KO mice.

These data suggest that MNCs isolated from PLCδ1 KO mice are unable to undergo osmotically evoked hypertrophy or osmotically induced ΔN-TRPV1 translocation. These data may provide an explanation for the dysfunctional systemic osmoregulation observed in PLCδ1 KO mice, which will be discussed in further detail in Chapter 6.

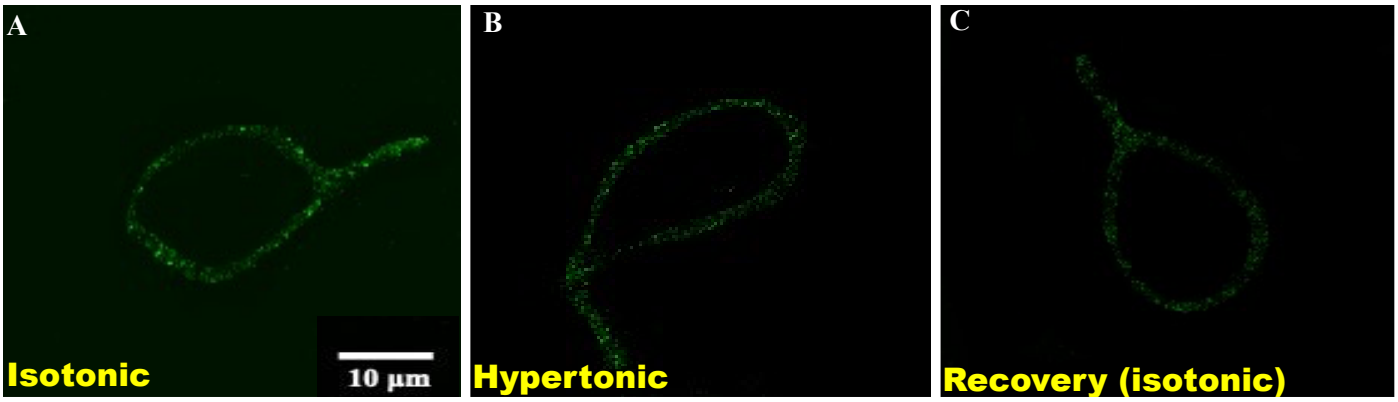

Figure 5.7: PLCδ1 KO mice do not display hypertrophy or ΔN-TRPV1 translocation in response increases in external osmolality. Representative immunocytochemistry images of the graphs presented in Figure 5.8 and Figure 5.9. (A) Isotonic treatment (310 ± 5 mosmol kg^{-1}). (B) Hypertonic treatment (340 ± 5 mosmol kg^{-1}). (C) Recovery treatment (hypertonic, then isotonic).

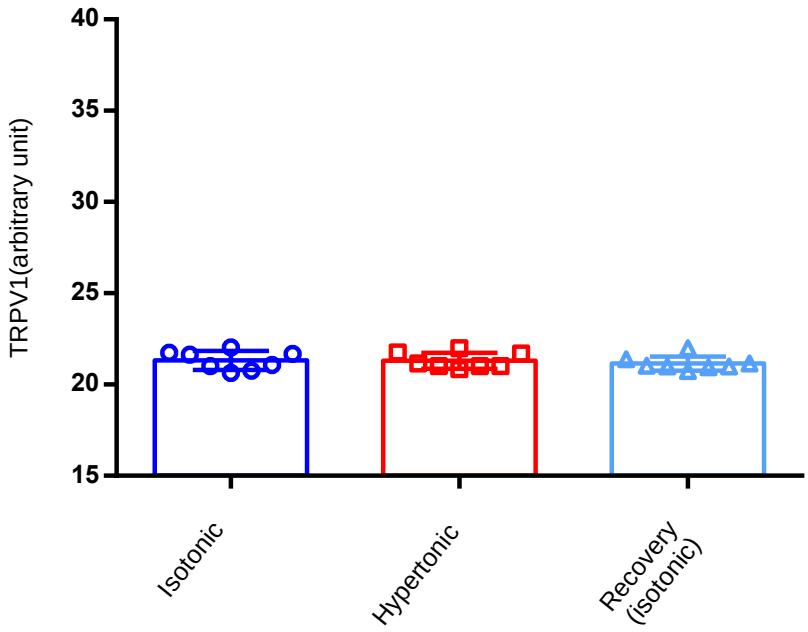

Figure 5.8: PLCδ1 KO mice are unable to respond to sustained increases in external osmolality through osmotically induced ΔN-TRPV1 translocation. Bar-scatter plot showing that PLCδ1 KO mice do not have the ability to increase the amount of TRPV1 present on the membrane in response to hypertonic solution, as there was no increase in TRPV1 immunofluorescence between isolated MNCs treated with isotonic or hypertonic solution (isotonic: 21.37 ± 0.5200, n= 8 to hypertonic: 21.31 ± 0.4385, n= 8, ns). There was also no change in TRPV1 labeling after washout of hypertonic solution with isotonic solution (hypertonic: 21.31 ± 0.4385, n= 8 to recovery: 21.15 ± 0.3823, n= 8, ns). F (2, 21) = 0.3480.

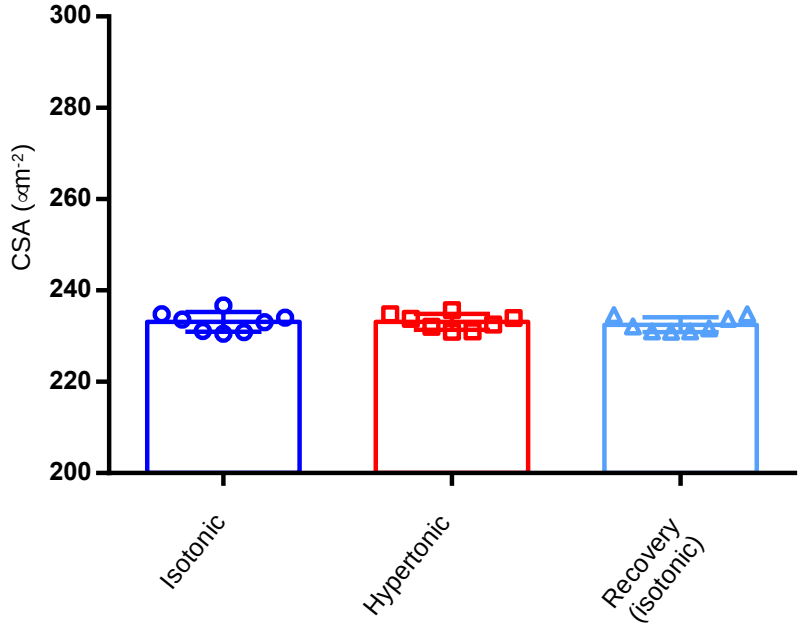

Figure 5.9: PLCδ1 KO mice do not display osmotically evoked increases in cross-sectional area (CSA). Bar-scatter plot showing that PLCδ1 KO mice do not have the ability to undergo hypertrophy in response to hypertonic solution, as there was no increase in MNC CSA between isolated MNCs treated with isotonic or hypertonic solution ((isotonic: 233.10 $\pm$ 2.1726 μm^2, n= 8 to hypertonic: 233.11 $\pm$ 1.7395 μm^2, n= 8, ns). There was also no change in CSA after washout of hypertonic solution with isotonic solution (hypertonic: 233.11 $\pm$ 1.7395 μm^2, n= 8 to recovery: 232.50 $\pm$ 1.6393 μm^2, n= 8, ns). F (2, 21) = 0.2799.

CHAPTER 6: DISCUSSION

The structural and functional adaptations of MNCs to sustained high osmolality include changes in plasma membrane protein levels and gene expression (Shuster et al., 1999; Tanaka et al., 1999; Ghorbel et al., 2003), as well as somatic hypertrophy (Modney and Hatton, 1989; Shah et al., 2014). Mammals are able to sustain high levels of VP release during periods of dehydration lasting days (Wakerly et al., 1978; Modney and Hatton, 1989). The mechanisms by which mammals are able to continually fire APs and release VP during periods of dehydration are poorly understood. Processes such as Na^+ channel translocation, increases in gene expression, and MNC hypertrophy are known to occur in response to sustained increases in external osmolality (Tanaka et al., 1999; Ghorbel et al., 2003; Miyata and Hatton, 2002; Shah et al., 2014), but it is not yet known why these processes exist. Because they do exist, they are likely to be physiologically relevant, and because they are different than the processes that regulate short-term osmoregulation, it is likely that different mechanisms regulate long-term osmoregulation in MNCs. We demonstrated that an osmotically induced translocation of ΔN-TRPV1 channels from internal stores to the MNC plasma membrane occurs, and that it operates through the same mechanisms as MNC hypertrophy *in vitro*, which will be discussed in further detail below. This finding suggests that ΔN-TRPV1 translocation may be a part of the structural and functional adaptations of MNCs to sustained increases in external osmolality, which may enable MNCs to sustain a high degree of AP firing and hormone release during periods of dehydration. It was also observed that both osmotically induced ΔN-TRPV1 translocation and osmotically evoked MNC hypertrophy require PLCδ1. This chapter will elaborate on the evidence presented in Chapter 5, and will discuss the possible physiological implications of osmotically induced ΔN-TRPV1 translocation in MNCs.

6.1 Osmotically induced increases in MNC plasma membrane ΔN-TRPV1 occur and are reversible

We show here that reversible osmotically induced increases in MNC plasma membrane ΔN-TRPV1 occur in parallel with osmotically evoked hypertrophy. Stimulating MNCs with hyperosmotic solution for a similar time course as previously described (Shah et al., 2014), we performed immunocytochemistry experiments to examine the effects of sustained increases in external osmolality on MNC plasma membrane ΔN-TRPV1 immunofluorescence in rats and mice. We report that there is a significant increase in membrane ΔN-TRPV1 immunofluorescence during sustained increases in osmolality (i.e., 1 hour). MNC hypertrophy also occurred during this time. Because MNC hypertrophy is a reversible process (Shah et al., 2014), we aimed to also examine whether the increase in plasma membrane ΔN-TRPV1 density was reversible. We also report that the osmotically induced increase in membrane ΔN-TRPV1 is reversible, as cells in the recovery treatment (see section 3.4.1) exhibited a return to isotonic levels of both ΔN-TRPV1 immunofluorescence and membrane area in rats (see Figure 5.1, Figure 5.2, and Figure 5.5) and in control mice (see Figure 5.3, Figure 5.4, and Figure 5.6). This may contribute to the ability of MNCs to sustain depolarizing currents over long periods of time, as an increased number of ΔN-TRPV1 channels on the plasma membrane could enhance MNC excitability.

6.2 PLC and PKC are required for the osmotically induced increase in plasma membrane ΔN-TRPV1

Because previous research suggested that PLC is involved in MNC hypertrophy (Shah et al., 2014) as well as TRPV1 translocation in other neurons (Jeske et al., 2009; Zhang et al., 2005), we next aimed to determine whether PLC is involved in the osmotically induced increase in ΔN-TRPV1. We examined the effects of hypertonic stimuli in the presence of the PLC inhibitor U-73122 (see section 3.4.2). We observed that despite being in a hypertonic solution the presence of the PLC inhibitor prevented the expected increase in both ΔN-TRPV1 immunofluorescence and membrane area (see Figure 5.1, Figure 5.2, and Figure 5.5), which suggests that PLC is required for the osmotically induced increase in both ΔN-TRPV1 immunofluorescence and membrane area.

Since PKC is activated downstream of PLC by DAG (Rhee, 2001), is required for MNC hypertrophy (Shah et al., 2014), and promotes increases in membrane TRPV1 expression and translocation in other neurons (Zhang et al., 2005; Malek et al., 2015), we sought next to determine whether PKC activation was required for the osmotically induced increase in membrane ΔN-TRPV1. Applying the PKC inhibitor bisindolylmaleimide in the presence of a hypertonic solution (see section 3.4.3) prevented an increase in both ΔN-TRPV1 immunofluorescence and membrane area (see Figure 5.1, Figure 5.2, and Figure 5.5), suggesting that PKC is necessary for the osmotically induced increase in both ΔN-TRPV1 immunofluorescence and membrane area.

6.3 Dynamin-mediated endocytosis is required for retrieval of ΔN-TRPV1 from the plasma membrane

Recovery from translocation has been shown to be dependent on dynamin-mediated endocytosis (Chen et al., 1991). The recovery from MNC hypertrophy is also dependent on dynamin-mediated endocytosis (Shah et al., 2014). Therefore, the next step in determining the mechanisms of the reversible osmotically induced increase in plasma membrane ΔN-TRPV1 was to determine whether the reversal of the increase we observed was due to dynamin-mediated endocytosis. By adding the dynamin inhibitor dynasore to the recovery treatment (see section 3.4.4) we observed that the recovery from hypertrophy was blocked. We also observed that dynasore prevented the decrease in plasma membrane ΔN-TRPV1 immunofluorescence that was observed in the recovery treatment without dynasore (see Figure 5.1, Figure 5.2, and Figure 5.5). This finding suggests that dynamin-mediated endocytosis is required for the reversal of the osmotically induced increase in membrane ΔN-TRPV1 immunofluorescence.

6.4 Vesicles from the Golgi are required for the osmotically induced increase in plasma membrane ΔN-TRPV1

Since movement of channel-containing vesicles derived from the Golgi to the plasma membrane are associated with translocation (Alberts et al., 2002), we aimed to determine the effect of inhibiting channel movement from the Golgi on osmotically induced plasma membrane ΔN-TRPV1 levels using the inhibitor peptide Exo-1 (Morgan and Burgoyne, 1992). Isolated MNCs exposed to a hypertonic solution containing Exo-1 (see section 3.4.5) showed no increase in either

ΔN-TRPV1 immunofluorescence or membrane area in rats (see Figure 5.1, Figure 5.2, and Figure 5.5) or in control mice (see Figure 5.3, Figure 5.4, and Figure 5.6), suggesting that movement of ΔN-TRPV1 from internally stored vesicles produced by the Golgi are required for the osmotically induced increase.

6.5 SNARE-mediated exocytosis is required for the osmotically induced increase in plasma membrane ΔN-TRPV1

Because SNARE-mediated exocytosis is required for MNC hypertrophy (Shah et al., 2014) and TRPV1 translocation (Planells-Cases et al., 2011; Camprubí-Robles et al., 2009), we next sought to determine whether SNARE-mediated exocytotic membrane fusion is required for the increase in plasma membrane ΔN-TRPV1. We treated MNCs exposed to hypertonic solution with the SNARE complex inhibitor TAT-NSF700 (see section 3.4.6), which inhibits NSF-mediated ATP hydrolysis and therefore vesicular membrane fusion, and observed that there was no increase in ΔN-TRPV1 immunofluorescence or membrane area (see Figure 5.1, Figure 5.2, and Figure 5.5; the membrane area experiment was previously conducted by Shah et al., 2014), suggesting that SNARE-mediated exocytotic fusion is required for the osmotically induced increase in membrane ΔN-TRPV1.

6.6 PLCδ1 is required for MNC hypertrophy as well as for the osmotically induced increase in plasma membrane ΔN-TRPV1

Previous data from our laboratory suggested that a Ca^{2+}-dependent isoform of PLC was required for osmotically evoked increases in ΔN-TRPV1 currents (Bansal and Fisher, 2017). We then determined that the PLCδ1 isoform modulates the increase in ΔN-TRPV1 currents (Park et al., 2021), and that mice void of this isoform exhibited dysfunctional systemic osmoregulation (Park et al., 2021). We therefore sought to determine whether PLCδ1 is the isoform responsible for the observed osmotically induced increase in ΔN-TRPV1 immunofluorescence. We repeated the initial experiments (see section 3.4.1) in PLCδ1 KO mice to observe whether an osmotically induced increase in ΔN-TRPV1 or membrane area occurred. We report that there is no osmotically induced increase in either ΔN-TRPV1 immunofluorescence or membrane area in PLCδ1 KO mice (see Figure 5.7, Figure 5.8, and Figure 5.9), suggesting that PLCδ1 is the isoform of PLC involved in mediating both increases in MNCs. Our data suggest that osmotically induced ΔN-TRPV1 translocation occurs in MNCs, and that the translocation is dependent on PLCδ1. Because PKC and SNARE-dependent exocytosis are both activated by PLC (Jeske et al., 2009; Zhang et al, 2005; Morenilla-Palao et al., 2004; Planells-Cases et al., 2011; Camprubí-Robles et al., 2009; Rhee, 2001; Sakai et al., 2010), we suggest that PLCδ1 could modulate the intracellular processes that lead to osmotically induced ΔN-TRPV1 translocation. This novel finding is important to our understanding of MNC osmoregulation. As illustrated by our laboratory in a recent study (Park et al., 2021), PLδ1 KO mice exhibit dysfunctional systemic osmoregulation as well as the inability to transduce changes in external osmolality into the depolarizing currents that lead to enhanced MNC AP firing and VP release. PLCδ1 could be responsible for modulating sustained increases

in osmosensory transduction and ΔN-TRPV1 current through its apparent effects on ΔN-TRPV1 translocation and MNC hypertrophy. These findings provide evidence for the physiological significance of PLCδ1 and its functions in osmoregulation.

6.7 Integration of short- and long-term adaptations of MNCs to hyperosmolality

6.7.1 Short-term processes mediated by PLCδ1 in response to hyperosmolality

When isolated MNCs are exposed to a hyperosmotic solution, they shrink (Oliet and Bourque, 1993). This shrinkage activates the mechanosensitive ΔN-TRPV1 channels and enables cation influx and depolarization of the MNC, therefore making it more likely to fire APs (Zaelzer et al., 2015). This depolarization activates L-type Ca^{2+} channels and enables Ca^{2+} influx (Zaelzer et al., 2015). We suggest that the increase in $[Ca^{2+}]_i$ that results from the Ca^{2+} influx then leads to the activation of PLCδ1. Once activated, PLCδ1 cleaves PIP_2 into IP_3 and DAG (for more information on PLC activation, see section 1.3.1.1; Rhee, 2001). Modulating PIP_2 levels can directly modulate TRPV1 activity in other neurons (Lukacs et al., 2007; Rohacs et al., 2008), so the increase in PIP_2 cleavage may also modulate ΔN-TRPV1 activity in MNCs. The PKC that is activated downstream by DAG could potentially phosphorylate ΔN-TRPV1 on the membrane and enhance their open probability, as has been shown in other neuron types (Premkumar and Ahern, 2000; Vellani et al., 2001). PKC activation could also enhance F-actin polymerization and further enhance the mechanosensitivity of membrane-bound ΔN-TRPV1 channels (Zhang et al., 2007b; Zhang and Bourque, 2008). The model described in section 1.6 explains in further detail how we suggest PLCδ1 modulates short-term MNC osmoregulation. We suggest a new mechanism below for the

long-term structural and functional adaptations of MNCs that we also believe to be mediated by PLCδ1.

6.7.2 Long-term responses of MNCs to hyperosmolality

The more rapid changes in MNCs described above do not provide a full explanation for the ability of MNCs to sustain a high degree of AP firing and hormone output in response to sustained increases in osmolality. Because MNCs undergo structural and functional adaptations in response to sustained increases in external osmolality (e.g., from dehydration), such as hypertrophy (Miyata and Hatton, 2002; Shah et al., 2014), upregulation of genes (Ghorbel et al., 2003), and increased membrane density of channels and receptors (Shuster et al., 1999; Tanaka et al., 1999; Hurbin et al., 2002), there are likely multiple processes that contribute to the adaptive responses of MNCs to sustained hyperosmolar exposure. It is not yet known exactly how MNCs adapt to sustained high osmolality, but our recent findings suggest that osmotically induced ΔN-TRPV1 translocation may be one adaptive mechanism. We also suggest based on the data presented in Chapter 5 that PLCδ1 also plays a role in triggering the long-term adaptations of MNCs to hyperosmolality.

6.8 Future directions

6.8.1 Electrophysiology

Electrophysiology is a powerful tool that could be used to observe what happens to ΔN-TRPV1 currents during sustained exposure to hyperosmolality. Based on the evidence presented in Chapter 5, we predict that there would be an increase in ΔN-TRPV1 currents because the osmotically induced ΔN-TRPV1 translocation increases plasma membrane ΔN-TRPV1 density. We have begun to test this hypothesis, and preliminary data from our laboratory have shown that there is an increase in ΔN-TRPV1 conductance with sustained exposure to hyperosmolality (Dr. Sung Jin Park, unpublished data). The increase in conductance could be due to an increase in ΔN-TRPV1 open probability. We have also performed immunocytochemistry and electrophysiology experiments to address this possibility and have found that after a 10-minute exposure to hyperosmolality, there is a significant increase in ΔN-TRPV1 conductance compared to cells that remained in isosmotic solution, but no significant increase in plasma membrane ΔN-TRPV1 density (Dr. Sung Jin Park and Kirk Haan, unpublished data). The increase in ΔN-TRPV1 conductance after 1 hour of exposure to hyperosmolality was significantly higher than the increase after 10 minutes. These data suggest that the initial increase in ΔN-TRPV1 conductance is due to an increase in open probability and not plasma membrane ΔN-TRPV1 density, but the sustained increase in ΔN-TRPV1 conductance is due to ΔN-TRPV1 translocation only. How ΔN-TRPV1 mechanosensitivity is affected after the addition of membrane to the cell surface during the hypertrophic process is unclear. A potential explanation to address this issue is presented in the paragraph below.

MNC hypertrophy could decrease the membrane stretch of MNCs. ΔN-TRPV1 on the MNC membrane could therefore become less active due to the mechanical gating nature of the channel (see section 1.2.5 for more information). During osmotically induced ΔN-TRPV1 translocation there is an increase in plasma membrane ΔN-TRPV1 density, which will increase conductance and depolarizing currents by itself. It is possible that during MNC hypertrophy, ΔN-TRPV1 current depends less on interactions with the cytoskeleton and more on other processes like translocation. ΔN-TRPV1 currents during hypertrophy may also be influenced by phosphorylation by PKC. Previous studies have shown that TRPV1 phosphorylation by PKC enhances its open probability (Premkumar and Ahern, 2000; Vellani et al., 2001). We have shown above that osmotically induced ΔN-TRPV1 translocation depends on PLCδ1 and PKC activation, so enhanced PKC activation in response to the enhanced osmotic activation of PLCδ1 could enhance the phosphorylation and therefore open probability of ΔN-TRPV1, which could lead to the increase in ΔN-TRPV1 current that we have observed. This explanation emphasizes the importance of translocation of ΔN-TRPV1 to the membrane, and the activation of PKC by PLCδ1 that could further enhance ΔN-TRPV1 currents and translocation of more ΔN-TRPV1 to the membrane.

6.8.2 *In vivo* experimentation

Since we have shown that osmotically induced ΔN-TRPV1 translocation occurs *in vitro*, a next step would be to examine how ΔN-TRPV1 translocation is important for osmoregulation *in vivo*. To explore this possibility, we could perform ΔN-TRPV1 immunocytochemistry and immunohistochemistry experiments on rats that have undergone a 24-hour period of dehydration,

as this period seemed to be sufficient to elicit a significant increase in blood osmolality in mice (Zerbe and Robertson, 1983; Zingg et al., 1986). We could use this period to examine how dehydration affects plasma membrane ΔN-TRPV1 density. We could also examine ΔN-TRPV1 currents in MNCs isolated from dehydrated rats that are placed in hyperosmotic solution using electrophysiology to determine whether similar currents observed using hyperosmotic stimulation *in vitro* would be observed using MNCs from dehydrated rats.

It would be of interest to attempt to block translocation *in vivo* by injecting inhibitors of translocation like Exo-1 and TAT-NSF700 (see section 3.3.4 and section 3.3.5 for more information on Exo-1 and TAT-NSF-700, respectively) into the SONs of rats that are being dehydrated and compare their blood osmolality to dehydrated rats injected with saline alone. From these experiments we could also examine MNC plasma membrane ΔN-TRPV1 density to observe whether administering a translocation inhibitor *in vivo* prevents osmotically induced ΔN-TRPV1 translocation, and whether that could be correlated with a more pronounced increase in serum osmolality like that observed in dehydrated PLCδ1 KO mice (Park et al., 2021). Observing ΔN-TRPV1 currents would also be of interest in MNCs isolated from dehydrated rats treated with Exo-1 or TAT-NSF700 *in vivo* to observe whether the presence of the translocation inhibitor diminishes osmotically evoked ΔN-TRPV1 currents.

It would also be of interest to determine the synaptotagmin isoform involved in osmotically induced ΔN-TRPV1 translocation (for more information on synaptotagmin and SNARE-mediated exocytosis, see section 1.4.1). Once we have identified the isoform, we could create an inducible KO model mouse for the synaptotagmin isoform to observe whether lacking the isoform elicits

any defects in systemic osmoregulation, MNC hypertrophy, or osmotically induced ΔN-TRPV1 translocation. The inducibility of the KO would also allow us to examine whether knocking the synaptotagmin back into function restores any degree of normal osmoregulation.

6.8.3 Transcription and translation in osmotically induced ΔN-TRPV1 translocation

Because dehydration lasting periods of days leads to changes in gene expression in MNCs (Ghorbel et al., 2003; Shuster et al., 1999), it is possible that ΔN-TRPV1 transcription and translation are also upregulated in MNCs during dehydration. The synthesis and packaging of new ΔN-TRPV1 into vesicles could potentially provide MNCs with a continual source of new ΔN-TRPV1 vesicles that could then be translocated to the MNC plasma membrane in addition to the pre-existing vesicles that apparently translocate to the membrane under osmotic stress. Sp1 and Sp4 are transcription factors that mediate TRPV1 transcription in other neurons (Chu et al., 2011). Sp4 expression is required for the persistence of hyperalgesia (Sheehan et al., 2019), and hyperalgesia requires TRPV1 (Davis et al., 2000). Mice that are hemizygous (+/-) for Sp4 do not display persistent hyperalgesia or an increase in mechanical hypersensitivity by TRPV1 (Sheehan et al., 2019), suggesting an intrinsic relationship between Sp4 expression and the expression of TRPV1. Sp1 and Sp4 are nuclear proteins that are activated through phosphorylation by PKC (You et al., 2007; Tan and Khachigian, 2009) in a Ca^{2+}-dependent manner (Chu et al., 2011). Sp1 and Sp4 are located on the GC box of the P2-promoter region of the TRPV1 gene (Chu et al., 2011), and once activated promote the transcription of TRPV1 mRNA (Chu et al., 2011) through RNA polymerase II activation (Dynan and Tjian, 1983). PKC has also been shown to enhance TRPV1 translation in other neurons (Kays et al., 2018). There is potential for these processes to be present

in MNCs, though it has not yet been examined. Because the transcription, translation, and translocation of TRPV1 requires PKC and Ca^{2+} in other neurons (Chu et al., 2011; You et al., 2007; Kays et al., 2018; Jeske et al., 2009; Zhang et al., 2005; Morenilla-Palao et al., 2004) and osmotically evoked hypertrophy requires PKC, Ca^{2+}, and changes in gene expression in MNCs (Shah et al., 2014; Ghorbel et al., 2003), it is possible that osmotically induced ΔN-TRPV1 transcription and translation could occur alongside osmotically induced ΔN-TRPV1 translocation in MNCs. If transcription and translation of new ΔN-TRPV1 channels plays a role in the long-term response of MNCs and coincides with ΔN-TRPV1 translocation, there is potential for PLCδ1 to also play a role in the synthesis of new ΔN-TRPV1. The osmotic stimulation of PLCδ1 that enhances PKC activity could influence the PKC-enabled transcription and translation of ΔN-TRPV1 channels.

CHAPTER 7: CONCLUSIONS

MNCs of the SON possess unique physiological adaptations to changes in external osmolality *in vivo* and *in vitro*. These physiological adaptations include changes in cell size, membrane channel and receptor density, protein expression, and electrical activity, some or all of which may contribute to the ability of MNCs to sustain a high degree of AP firing and hormone release under long-term hyperosmotic stress. We have shown a novel mechanism of reversible, osmotically induced ΔN-TRPV1 translocation to the MNC plasma membrane from internal stores in isolated MNCs, which also accompanies hypertrophy in response to sustained hyperosmolar exposure. We have also shown that the osmotically induced increase in plasma ΔN-TRPV1 levels requires the activation of both PLC and PKC, as well as SNARE-mediated exocytosis and vesicular transport from the Golgi. Furthermore, the reversal of the osmotically induced increase in plasma membrane ΔN-TRPV1 that occurs once a hyperosmotic stimulus is removed requires dynamin-mediated endocytosis. Lastly, we have shown that mice that lack PLCδ1 do not possess the ability to increase MNC size or plasma membrane ΔN-TRPV1 levels in response to hyperosmolality, suggesting that it is the PLC isoform involved in mediating osmotically induced ΔN-TRPV1 translocation and MNC hypertrophy. In the future, we would like to further examine the electrophysiological implications of ΔN-TRPV1 translocation (as outlined in section 6.8.1), as well as explore osmotically induced ΔN-TRPV1 translocation *in vivo* and the possibility of the involvement of transcription and translation in the process (as outlined in section 6.8.2 and section 6.8.3, respectively). These findings further elucidate the mechanisms of MNC hypertrophy and osmoregulation in mammals and provide an explanation for the sustained AP firing of and hormone release from MNCs of water-deprived or dehydrated mammals.

CHAPTER 8: REFERENCES

Agre P. The aquaporin water channels. *Proc Am Thorac Soc* 3: 5–13, 2006.

Akaishi T, **Negoro H**, **Kobayasi S**. Responses of paraventricular and supraoptic units to angiotensin II, Sar1-Ile8-angiotensin II and hypertonic NaCl administered into the cerebral ventricle [Online]. *Brain Res* , 1980https://www.sciencedirect.com/science/article/pii/0006899380900487.

Alberts B, **Johnson A**, **Lewis J**, **Raff M**, **Roberts K**, **Walter P**. *Transport from the ER through the Golgi Apparatus*. Garland Science, 2002.

Allen V, **Swigart P**, **Cheung R**, **Cockcroft S**, **Katan M**. Regulation of inositol lipid-specific phospholipase cdelta by changes in Ca2+ ion concentrations. *Biochem J* 327 (Pt 2): 545–552, 1997.

Anderson JW, **Washburn DL**, **Ferguson AV**. Intrinsic osmosensitivity of subfornical organ neurons. *Neuroscience* 100: 539–547, 2000.

Andrew RD, **Dudek FE**. Analysis of intracellularly recorded phasic bursting by mammalian neuroendocrine cells. *J Neurophysiol* 51: 552–566, 1984.

Antunes VR. Hypertonic NaCl versus osmotic stimuli: distinct OVLT neurones can sense the difference to control sympathetic outflow and blood pressure. *J. Physiol.* 595: 6089–6090, 2017.

Armstrong WE, **Schöler J**, **McNeill TH**. Immunocytochemical, Golgi and electron microscopic characterization of putative dendrites in the ventral glial lamina of the rat supraoptic nucleus. *Neuroscience* 7: 679–694, 1982a.

Armstrong WE, **Sladek CD**, **Sladek JR Jr**. Characterization of noradrenergic control of vasopressin release by the organ-cultured rat hypothalamo-neurohypophyseal system. *Endocrinology* 111: 273–279, 1982b.

Armstrong WE. Morphological and electrophysiological classification of hypothalamic supraoptic neurons. *Prog Neurobiol* 47: 291–339, 1995.

Austin CP, **Battey JF**, **Bradley A**, **Bucan M**, **Capecchi M**, **Collins FS**, **Dove WF**, **Duyk G**, **Dymecki S**, **Eppig JT**, **Grieder FB**, **Heintz N**, **Hicks G**, **Insel TR**, **Joyner A**, **Koller BH**, **Lloyd KCK**, **Magnuson T**, **Moore MW**, **Nagy A**, **Pollock JD**, **Roses AD**, **Sands AT**, **Seed B**, **Skarnes WC**, **Snoddy J**, **Soriano P**, **Stewart DJ**, **Stewart F**, **Stillman B**, **Varmus H**, **Varticovski L**, **Verma IM**, **Vogt TF**, **von Melchner H**, **Witkowski J**, **Woychik RP**, **Wurst W**, **Yancopoulos GD**, **Young SG**, **Zambrowicz B**. The knockout mouse project. *Nat Genet* 36: 921–924, 2004.

Ayus JC, **Varon J**, **Arieff AI**. Hyponatremia, cerebral edema, and noncardiogenic pulmonary

edema in marathon runners. *Ann Intern Med* 132: 711–714, 2000.

Baertschi AJ, **Vallet PG**. Osmosensitivity of the hepatic portal vein area and vasopressin release in rats. *J Physiol* 315: 217–230, 1981.

Ball SG. Vasopressin and disorders of water balance: the physiology and pathophysiology of vasopressin. *Ann Clin Biochem* 44: 417–431, 2007.

Bankir L, **Bouby N**, **Trinh-Trang-Tan M-M**. 2 The role of the kidney in the maintenance of water balance. *Baillieres Clin Endocrinol Metab* 3: 249–311, 1989.

Bansal V, **Fisher TE**. Osmotic activation of a Ca2+-dependent phospholipase C pathway that regulatesΔ N TRPV1-mediated currents in rat supraoptic neurons. *Physiological reports* 5: e13259, 2017.

Battey NH, **James NC**, **Greenland AJ**, **Brownlee C**. Exocytosis and endocytosis. *Plant Cell* 11: 643–660, 1999.

Baxter DA, **Byrne JH**. Ionic conductance mechanisms contributing to the electrophysiological properties of neurons. *Curr Opin Neurobiol* 1: 105–112, 1991.

Beagley GH, **Hatton GI**. Rapid morphological changes in supraoptic nucleus and posterior pituitary induced by a single hypertonie saline injection. *Brain Res Bull* 28: 613–618, 1992.

Bell RM. Protein kinase C activation by diacylglycerol second messengers. *Cell* 45: 631–632, 1986.

Bennett GJ, **Xie YK**. A peripheral mononeuropathy in rat that produces disorders of pain sensation like those seen in man. *Pain* 33: 87–107, 1988.

Bhave G, **Zhu W**, **Wang H**, **Brasier DJ**, **Oxford GS**, **Gereau RW 4th**. cAMP-dependent protein kinase regulates desensitization of the capsaicin receptor (VR1) by direct phosphorylation. *Neuron* 35: 721–731, 2002.

Bicknell RJ, **Leng G**. Relative efficiency of neural firing patterns for vasopressin release in vitro. *Neuroendocrinology* 33: 295–299, 1981.

Bicknell RJ. Optimizing release from peptide hormone secretory nerve terminals. *J Exp Biol* 139: 51–65, 1988.

Bie P, **Wamberg S**, **Kjolby M**. Volume natriuresis vs. pressure natriuresis. *Acta Physiol Scand* 181: 495–503, 2004.

Blackburn RE, **Samson WK**, **Fulton RJ**, **Stricker EM**, **Verbalis JG**. Central oxytocin inhibition of salt appetite in rats: evidence for differential sensing of plasma sodium and osmolality. *Proc Natl Acad Sci U S A* 90: 10380–10384, 1993.

Blackburn RE, **Samson WK**, **Fulton RJ**, **Stricker EM**, **Verbalis JG**. Central oxytocin and ANP receptors mediate osmotic inhibition of salt appetite in rats. *Am J Physiol* 269: R245–51, 1995.

Blaicher W, **Gruber D**, **Bieglmayer C**, **Blaicher AM**, **Knogler W**, **Huber JC**. The role of oxytocin in relation to female sexual arousal. *Gynecol Obstet Invest* 47: 125–126, 1999.

Boron WF, **Boulpaep EL**. Medical Physiology: Filadelfia (Pensilvania, Estados Unidos) Editorial. Amsterdam: Elsevier2017.

Bourque CW, **Ciura S**, **Trudel E**, **Stachniak TJE**, **Sharif-Naeini R**. Neurophysiological characterization of mammalian osmosensitive neurones. *Exp Physiol* 92: 499–505, 2007.

Bourque CW, **Oliet SH**, **Richard D**. Osmoreceptors, osmoreception, and osmoregulation. *Front Neuroendocrinol* 15: 231–274, 1994.

Bourque CW, **Oliet SH**. Osmoreceptors in the central nervous system. *Annu Rev Physiol* 59: 601–619, 1997.

Bourque CW, **Voisin DL**, **Chakfe Y**. Stretch-inactivated cation channels: cellular targets for modulation of osmosensitivity in supraoptic neurons. *Prog Brain Res* 139: 85–94, 2002.

Bourque CW. Central mechanisms of osmosensation and systemic osmoregulation. *Nat Rev Neurosci* 9: 519–531, 2008.

Brown CH, **Bains JS**, **Ludwig M**, **Stern JE**. Physiological regulation of magnocellular neurosecretory cell activity: integration of intrinsic, local and afferent mechanisms. *J Neuroendocrinol* 25: 678–710, 2013.

Brown CH, **Bourque CW**. Autocrine feedback inhibition of plateau potentials terminates phasic bursts in magnocellular neurosecretory cells of the rat supraoptic nucleus. *J Physiol* 557: 949–960, 2004.

Brown CH, **Bourque CW**. Mechanisms of rhythmogenesis: insights from hypothalamic vasopressin neurons. *Trends Neurosci* 29: 108–115, 2006.

Brownstein MJ, **Russell JT**, **Gainer H**. Synthesis, transport, and release of posterior pituitary hormones. *Science* 207: 373–378, 1980.

Buggy J, **Hoffman WE**, **Phillips MI**, **Fisher AE**, **Johnson AK**. Osmosensitivity of rat third ventricle and interactions with angiotensin. *Am J Physiol* 236: R75–82, 1979.

Buggy J, **Jonhson AK**. Preoptic-hypothalamic periventricular lesions: thirst deficits and hypernatremia. *Am J Physiol* 233: R44–52, 1977.

Burbach JP, **Luckman SM**, **Murphy D**, **Gainer H**. Gene regulation in the magnocellular hypothalamo-neurohypophysial system. *Physiol Rev* 81: 1197–1267, 2001.

Burgoyne RD, **Morgan A**. Regulated exocytosis. *Biochem J* 293 (Pt 2): 305–316, 1993.

Calvert JW, **Gundewar S**, **Yamakuchi M**, **Park PC**, **Baldwin WM 3rd**, **Lefer DJ**, **Lowenstein CJ**. Inhibition of N-ethylmaleimide-sensitive factor protects against myocardial ischemia/reperfusion injury. *Circ Res* 101: 1247–1254, 2007.

Camprubí-Robles M, **Planells-Cases R**, **Ferrer-Montiel A**. Differential contribution of SNARE-dependent exocytosis to inflammatory potentiation of TRPV1 in nociceptors. *FASEB J* 23: 3722–3733, 2009.

Carlson SH, **Beitz A**, **Osborn JW**. Intragastric hypertonic saline increases vasopressin and central Fos immunoreactivity in conscious rats. *Am J Physiol* 272: R750–8, 1997.

Carroll RC, **Beattie EC**, **von Zastrow M**, **Malenka RC**. Role of AMPA receptor endocytosis in synaptic plasticity. *Nat Rev Neurosci* 2: 315–324, 2001.

Caterina MJ, **Schumacher MA**, **Tominaga M**, **Rosen TA**, **Levine JD**, **Julius D**. The capsaicin receptor: a heat-activated ion channel in the pain pathway. *Nature* 389: 816–824, 1997.

Ceccarelli B, **Hurlbut WP**, **Mauro A**. Turnover of transmitter and synaptic vesicles at the frog neuromuscular junction. *J Cell Biol* 57: 499–524, 1973.

Chakfe Y, **Bourque CW**. Excitatory peptides and osmotic pressure modulate mechanosensitive cation channels in concert. *Nature Neuroscience* 3: 572–579, 2000.

Chamberlin ME, **Strange K**. Anisosmotic cell volume regulation: a comparative view. *Am J Physiol* 257: C159–73, 1989.

Chavkin C, **James IF**, **Goldstein A**. Dynorphin is a specific endogenous ligand of the kappa opioid receptor. *Science* 215: 413–415, 1982.

Chen MS, **Obar RA**, **Schroeder CC**, **Austin TW**, **Poodry CA**, **Wadsworth SC**, **Vallee RB**. Multiple forms of dynamin are encoded by shibire, a Drosophila gene involved in endocytosis. *Nature* 351: 583–586, 1991.

Chen YA, **Scheller RH**. SNARE-mediated membrane fusion. *Nat Rev Mol Cell Biol* 2: 98–106, 2001.

Chu C, **Zavala K**, **Fahimi A**, **Lee J**, **Xue Q**, **Eilers H**, **Schumacher MA**. Transcription factors Sp1 and Sp4 regulate TRPV1 gene expression in rat sensory neurons. *Mol Pain* 7: 44, 2011.

Ciura S, **Bourque CW**. Transient Receptor Potential Vanilloid 1 Is Required for Intrinsic Osmoreception in Organum Vasculosum Lamina Terminalis Neurons and for Normal Thirst

Responses to Systemic Hyperosmolality. *J Neurosci* 26: 9069–9075, 2006.

Clapham DE. TRP channels as cellular sensors. *Nature* 426: 517–524, 2003.

Cocucci E, **Lorusso A**, **Ongania GN**, **Klajn A**, **Meldolesi J**. Non-secretory exocytoses in the brain. *J Physiol Paris* 99: 140–145, 2006.

Curran PF, **Solomon AK**. Ion and water fluxes in the ileum of rats. *J Gen Physiol* 41: 143–168, 1957.

Damke H, **Baba T**, **Warnock DE**, **Schmid SL**. Induction of mutant dynamin specifically blocks endocytic coated vesicle formation. *J Cell Biol* 127: 915–934, 1994.

Davis JB, **Gray J**, **Gunthorpe MJ**, **Hatcher JP**, **Davey PT**, **Overend P**, **Harries MH**, **Latcham J**, **Clapham C**, **Atkinson K**, **Hughes SA**, **Rance K**, **Grau E**, **Harper AJ**, **Pugh PL**, **Rogers DC**, **Bingham S**, **Randall A**, **Sheardown SA**. Vanilloid receptor-1 is essential for inflammatory thermal hyperalgesia. *Nature* 405: 183–187, 2000.

Dutton A, **Dyball RE**. Phasic firing enhances vasopressin release from the rat neurohypophysis. *J Physiol* 290: 433–440, 1979.

Dynan WS, **Tjian R**. Isolation of transcription factors that discriminate between different promoters recognized by RNA polymerase II. *Cell* 32: 669–680, 1983.

Egan G, **Silk T**, **Zamarripa F**, **Williams J**, **Federico P**, **Cunnington R**, **Carabott L**, **Blair-West J**, **Shade R**, **McKinley M**, **Farrell M**, **Lancaster J**, **Jackson G**, **Fox P**, **Denton D**. Neural correlates of the emergence of consciousness of thirst. *Proc Natl Acad Sci U S A* 100: 15241–15246, 2003.

Emmeluth C, **Goetz KL**, **Drummer C**, **Gerzer R**, **Forssmann WG**, **Bie P**. Natriuresis caused by increased carotid Na+ concentration after renal denervation. *Am J Physiol* 270: F510–7, 1996.

Erstad BL. Osmolality and osmolarity: narrowing the terminology gap. *Pharmacotherapy* 23: 1085–1086, 2003.

Essen LO, **Perisic O**, **Cheung R**, **Katan M**, **Williams RL**. Crystal structure of a mammalian phosphoinositide-specific phospholipase C delta. *Nature* 380: 595–602, 1996.

Feng Y, **Yu S**, **Lasell TKR**, **Jadhav AP**, **Macia E**, **Chardin P**, **Melancon P**, **Roth M**, **Mitchison T**, **Kirchhausen T**. Exo1: a new chemical inhibitor of the exocytic pathway. *Proc Natl Acad Sci U S A* 100: 6469–6474, 2003.

Ferguson SM, **Brasnjo G**, **Hayashi M**, **Wölfel M**, **Collesi C**, **Giovedi S**, **Raimondi A**, **Gong L-W**, **Ariel P**, **Paradise S**, **O'toole E**, **Flavell R**, **Cremona O**, **Miesenböck G**, **Ryan TA**, **De Camilli P**. A selective activity-dependent requirement for dynamin 1 in synaptic vesicle endocytosis. *Science* 316: 570–574, 2007.

Ferguson SM, **De Camilli P**. Dynamin, a membrane-remodelling GTPase. *Nat Rev Mol Cell Biol* 13: 75–88, 2012.

Fineberg SK, **Ross DA**. Oxytocin and the Social Brain. *Biol Psychiatry* 81: e19–e21, 2017.

Fisher TE, **Bourque CW**. The function of Ca2+ channel subtypes in exocytotic secretion: new perspectives from synaptic and non-synaptic release. *Prog Biophys Mol Biol* 77: 269–303, 2001.

Fleischhauer J, **Lehmann L**, **Kléber AG**. Electrical resistances of interstitial and microvascular space as determinants of the extracellular electrical field and velocity of propagation in ventricular myocardium. *Circulation* 92: 587–594, 1995.

Ford MGJ, **Jenni S**, **Nunnari J**. The crystal structure of dynamin. *Nature* 477: 561–566, 2011.

Fortney SM, **Wenger CB**, **Bove JR**, **Nadel ER**. Effect of hyperosmolality on control of blood flow and sweating. *J Appl Physiol* 57: 1688–1695, 1984.

Fukami K, **Nakao K**, **Inoue T**, **Kataoka Y**. Requirement of phospholipase Cδ4 for the zona pellucida-induced acrosome reaction [Online]. 2001https://science.sciencemag.org/content/292/5518/920.abstract?casa_token=Biv-b5pGmfAAAAAA:8G2c_4XiBy_zlMnvpTtVk-9Kl_jmKIJZ6t6gphcrBUUkXF4I5IxnfIVHTzxt8BhJQQz1InnkJCLR.

Fyhrquist F, **Metsärinne K**, **Tikkanen I**. Role of angiotensin II in blood pressure regulation and in the pathophysiology of cardiovascular disorders. *J Hum Hypertens* 9 Suppl 5: S19–24, 1995.

Gauer OH, **Henry JP**, **Behn C**. The regulation of extracellular fluid volume. *Annu Rev Physiol* 32: 547–595, 1970.

Ghamari-Langroudi M, **Bourque CW**. Excitatory role of the hyperpolarization-activated inward current in phasic and tonic firing of rat supraoptic neurons. *J Neurosci* 20: 4855–4863, 2000.

Ghorbel MT, **Sharman G**, **Leroux M**, **Barrett T**, **Donovan DM**, **Becker KG**, **Murphy D**. Microarray analysis reveals interleukin-6 as a novel secretory product of the hypothalamo-neurohypophyseal system. *J Biol Chem* 278: 19280–19285, 2003.

Gizowski C, **Bourque CW**. The neural basis of homeostatic and anticipatory thirst. *Nat Rev Nephrol* 14: 11–25, 2018.

Glasgow E, **Murase T**, **Zhang B**, **Verbalis JG**, **Gainer H**. Gene expression in the rat supraoptic nucleus induced by chronic hyperosmolality versus hyposmolality. *Am J Physiol Regul Integr Comp Physiol* 279: R1239–50, 2000.

Gregory WA, **Tweedle CD**, **Hatton GI**. Ultrastructure of neurons in the paraventricular nucleus of normal, dehydrated and rehydrated rats. *Brain Res Bull* 5: 301–306, 1980.

Grinstein S, **Foskett JK**. Ionic mechanisms of cell volume regulation in leukocytes. *Annu Rev Physiol* 52: 399–414, 1990.

Gupta J, **Russell RJ**, **Wayman CP**, **Hurley D**, **Jackson VM**. Oxytocin-induced contractions within rat and rabbit ejaculatory tissues are mediated by vasopressin V1A receptors and not oxytocin receptors. *British Journal of Pharmacology* 155: 118–126, 2008.

Guyton AC, **Hall JE**. Textbook of medical physiology: Elsevier Saunders. *United States of America* 323, 2006.

Halperin ML, **Skorecki KL**. Interpretation of the urine electrolytes and osmolality in the regulation of body fluid tonicity. *Am J Nephrol* 6: 241–245, 1986.

Hanslick JL, **Lau K**, **Noguchi KK**, **Olney JW**, **Zorumski CF**, **Mennerick S**, **Farber NB**. Dimethyl sulfoxide (DMSO) produces widespread apoptosis in the developing central nervous system. *Neurobiol Dis* 34: 1–10, 2009.

Hatton GI. Emerging concepts of structure-function dynamics in adult brain: the hypothalamo-neurohypophysial system. *Prog Neurobiol* 34: 437–504, 1990.

Hatton GI. Function-related plasticity in hypothalamus. *Annu Rev Neurosci* 20: 375–397, 1997.

Hazell GGJ, **Hindmarch CC**, **Pope GR**, **Roper JA**, **Lightman SL**, **Murphy D**, **O'Carroll A-M**, **Lolait SJ**. G protein-coupled receptors in the hypothalamic paraventricular and supraoptic nuclei--serpentine gateways to neuroendocrine homeostasis. *Front Neuroendocrinol* 33: 45–66, 2012.

Henley JR, **Krueger EW**, **Oswald BJ**, **McNiven MA**. Dynamin-mediated internalization of caveolae. *J Cell Biol* 141: 85–99, 1998.

Heuser JE, **Reese TS**. Structural changes after transmitter release at the frog neuromuscular junction. *J Cell Biol* 88: 564–580, 1981.

Hille B. *Ionic Channels of Excitable Membranes*. Sinauer, 2001.

Ho KW, **Ward NJ**, **Calkins DJ**. TRPV1: a stress response protein in the central nervous system. *Am J Neurodegener Dis* 1: 1–14, 2012.

Hodgkin AL, **Huxley AF**. A quantitative description of membrane current and its application to conduction and excitation in nerve. *J Physiol* 117: 500–544, 1952.

Hoffmann EK, **Lambert IH**, **Pedersen SF**. Physiology of cell volume regulation in vertebrates. *Physiol Rev* 89: 193–277, 2009.

Huang W, **Lee SL**, **Arnason SS**, **Sjöquist M**. Dehydration natriuresis in male rats is mediated by oxytocin. *Am J Physiol* 270: R427–33, 1996.

Hurbin A, **Orcel H**, **Alonso G**, **Moos F**, **Rabié A**. The vasopressin receptors colocalize with vasopressin in the magnocellular neurons of the rat supraoptic nucleus and are modulated by water balance. *Endocrinology* 143: 456–466, 2002.

Jeske NA, **Patwardhan AM**, **Henry MA**, **Milam SB**. Fibronectin stimulates TRPV1 translocation in primary sensory neurons. *J Neurochem* 108: 591–600, 2009.

Jewell PA, **Verney EB**. An experimental attempt to determine the site of the neurohypophysial and osmoreceptors in the dog. *Philos trans R Soc Lond* 240: 197–324, 1957.

Jhamandas JH, **Lind RW**, **Renaud LP**. Angiotensin II may mediate excitatory neurotransmission from the subfornical organ to the hypothalamic supraoptic nucleus: an anatomical and electrophysiological study in the rat. *Brain Research* 487: 52–61, 1989.

Jimah JR, **Hinshaw JE**. Structural Insights into the Mechanism of Dynamin Superfamily Proteins. *Trends Cell Biol* 29: 257–273, 2019.

Kadamur G, **Ross EM**. Mammalian phospholipase C. *Annu Rev Physiol* 75: 127–154, 2013.

Kays J, **Zhang YH**, **Khorodova A**, **Strichartz G**, **Nicol GD**. Peripheral Synthesis of an Atypical Protein Kinase C Mediates the Enhancement of Excitability and the Development of Mechanical Hyperalgesia Produced by Nerve Growth Factor. *Neuroscience* 371: 420–432, 2018.

Kedei N, **Szabo T**, **Lile JD**, **Treanor JJ**, **Olah Z**, **Iadarola MJ**, **Blumberg PM**. Analysis of the native quaternary structure of vanilloid receptor 1. *J Biol Chem* 276: 28613–28619, 2001.

Knepper MA, **Kwon T-H**, **Nielsen S**. Molecular Physiology of Water Balance. *N. Engl. J. Med.* 373: 196, 2015.

Koenig JH, **Ikeda K**. Disappearance and reformation of synaptic vesicle membrane upon transmitter release observed under reversible blockage of membrane retrieval. *J Neurosci* 9: 3844–3860, 1989.

Lan JY, **Skeberdis VA**, **Jover T**, **Grooms SY**, **Lin Y**, **Araneda RC**, **Zheng X**, **Bennett MV**, **Zukin RS**. Protein kinase C modulates NMDA receptor trafficking and gating. *Nat Neurosci* 4: 382–390, 2001.

Lang F, **Busch GL**, **Völkl H**. The diversity of volume regulatory mechanisms. *Cell Physiol Biochem* 8: 1–45, 1998.

Lang F. Mechanisms and significance of cell volume regulation. *J Am Coll Nutr* 26: 613S–623S, 2007.

Lee WK, **Kim JK**, **Seo M-S**, **Cha J-H**, **Lee KJ**, **Rha HK**, **Min DS**, **Jo Y-H**, **Lee K-H**. Molecular Cloning and Expression Analysis of a Mouse Phospholipase C-δ1. *Biochem Biophys Res Commun* 261: 393–399, 1999.

Li Z, **Ferguson AV**. Angiotensin II responsiveness of rat paraventricular and subfornical organ neurons in vitro. *Neuroscience* 55: 197–207, 1993.

Liamis G, **Tsimihodimos V**, **Doumas M**, **Spyrou A**, **Bairaktari E**, **Elisaf M**. Clinical and laboratory characteristics of hypernatraemia in an internal medicine clinic. *Nephrol Dial Transplant* 23: 136–143, 2008.

Liu Y-W, **Neumann S**, **Ramachandran R**, **Ferguson SM**, **Pucadyil TJ**, **Schmid SL**. Differential curvature sensing and generating activities of dynamin isoforms provide opportunities for tissue-specific regulation. *Proc Natl Acad Sci U S A* 108: E234–42, 2011.

Logan MR, **Mandato CA**. Regulation of the actin cytoskeleton by PIP2 in cytokinesis. *Biol Cell* 98: 377–388, 2006.

Luby-Phelps K. Cytoarchitecture and physical properties of cytoplasm: volume, viscosity, diffusion, intracellular surface area. *Int Rev Cytol* 192: 189–221, 2000.

Ludwig M. Dendritic release of vasopressin and oxytocin. *J Neuroendocrinol* 10: 881–895, 1998.

Lukacs V, **Thyagarajan B**, **Varnai P**, **Balla A**, **Balla T**, **Rohacs T**. Dual regulation of TRPV1 by phosphoinositides. *J Neurosci* 27: 7070–7080, 2007.

Macia E, **Ehrlich M**, **Massol R**, **Boucrot E**, **Brunner C**, **Kirchhausen T**. Dynasore, a cell-permeable inhibitor of dynamin. *Dev Cell* 10: 839–850, 2006.

Malek N, **Pajak A**, **Kolosowska N**, **Kucharczyk M**, **Starowicz K**. The importance of TRPV1-sensitisation factors for the development of neuropathic pain. *Mol Cell Neurosci* 65: 1–10, 2015.

Maresh CM, **Herrera-Soto JA**, **Armstrong LE**, **Casa DJ**, **Kavouras SA**, **Hacker FT Jr**, **Elliott TA**, **Stoppani J**, **Scheett TP**. Perceptual responses in the heat after brief intravenous versus oral rehydration. *Med Sci Sports Exerc* 33: 1039–1045, 2001.

Marzban F, **Tweedle CD**, **Hatton GI**. Reevaluation of the plasticity in the rat supraoptic nucleus after chronic dehydration using immunogold for oxytocin and vasopressin at the ultrastructural level. *Brain Res Bull* 28: 757–766, 1992.

Matsushita K, **Morrell CN**, **Lowenstein CJ**. A novel class of fusion polypeptides inhibits exocytosis. *Mol Pharmacol* 67: 1137–1144, 2005.

McLaughlin S, **Wang J**, **Gambhir A**, **Murray D**. PIP2 and Proteins: Interactions,

Organization, and Information Flow. 2003. doi:10.1146/annurev.biophys.31.082901.134259.

Miaczynska M, **Stenmark H**. Mechanisms and functions of endocytosis. *J Cell Biol* 180: 7–11, 2008.

Michael J. Sanger, **Dorothy M. Brecheisen**, **Hynek BM**. Can Computer Animations Affect College Biology Students' Conceptions about Diffusion & Osmosis? *Am Biol Teach* 63: 104–109, 2001.

Miyata S, **Hatton GI**. Activity-related, dynamic neuron-glial interactions in the hypothalamo-neurohypophysial system. *Microsc Res Tech* 56: 143–157, 2002.

Modney BK, **Hatton GI**. Multiple synapse formation: a possible compensatory mechanism for increased cell size in rat supraoptic nucleus. *J Neuroendocrinol* 1: 21–27, 1989.

Montana V, **Liu W**, **Mohideen U**, **Parpura V**. Single molecule measurements of mechanical interactions within ternary SNARE complexes and dynamics of their disassembly: SNAP25 vs. SNAP23. *J Physiol* 587: 1943–1960, 2009.

Montell C. Physiology, phylogeny, and functions of the TRP superfamily of cation channels. *Sci STKE* 2001: re1, 2001.

Montell C. The TRP superfamily of cation channels. *Sci STKE* 2005: re3, 2005.

Moon RC, **Turner CW**. Effect of reserpine on oxytocin and lactogen discharge in lactating rats. *Proc Soc Exp Biol Med* 101: 332–335, 1959.

Morenilla-Palao C, **Planells-Cases R**, **García-Sanz N**, **Ferrer-Montiel A**. Regulated exocytosis contributes to protein kinase C potentiation of vanilloid receptor activity. *J Biol Chem* 279: 25665–25672, 2004.

Morgan A, **Burgoyne RD**. Interaction between protein kinase C and Exo1 (14-3-3 protein) and its relevance to exocytosis in permeabilized adrenal chromaffin cells. *Biochem J* 286 (Pt 3): 807–811, 1992.

Morita H, **Ogino T**, **Fujiki N**, **Tanaka K**, **Gotoh TM**, **Seo Y**, **Takamata A**, **Nakamura S**, **Murakami M**. Sequence of forebrain activation induced by intraventricular injection of hypertonic NaCl detected by Mn2+ contrasted T1-weighted MRI. *Auton Neurosci* 113: 43–54, 2004.

Morris M, **Li P**, **Callahan MF**, **Oliverio MI**, **Coffman TM**, **Bosch SM**, **Diz DI**. Neuroendocrine effects of dehydration in mice lacking the angiotensin AT1a receptor. *Hypertension* 33: 482–486, 1999.

Murphy MR, **Seckl JR**, **Burton S**, **Checkley SA**, **Lightman SL**. Changes in oxytocin and vasopressin secretion during sexual activity in men. *J Clin Endocrinol Metab* 65: 738–741, 1987.

Nakamura Y, **Fukami K**, **Yu H**, **Takenaka K**, **Kataoka Y**, **Shirakata Y**, **Nishikawa S-I**, **Hashimoto K**, **Yoshida N**, **Takenawa T**. Phospholipase Cdelta1 is required for skin stem cell lineage commitment. *EMBO J* 22: 2981–2991, 2003.

Nakamura Y, **Fukami K**. Regulation and physiological functions of mammalian phospholipase C. *J Biochem* 161: 315–321, 2017.

Nakata T, **Iwamoto A**, **Noda Y**, **Takemura R**, **Yoshikura H**, **Hirokawa N**. Predominant and developmentally regulated expression of dynamin in neurons. *Neuron* 7: 461–469, 1991.

Newton AC. Protein kinase C: structural and spatial regulation by phosphorylation, cofactors, and macromolecular interactions. *Chem Rev* 101: 2353–2364, 2001.

Niermann H, **Amiry-Moghaddam M**, **Holthoff K**, **Witte OW**, **Ottersen OP**. A novel role of vasopressin in the brain: modulation of activity-dependent water flux in the neocortex. *J Neurosci* 21: 3045–3051, 2001.

Oliet SH, **Bourque CW**. Properties of supraoptic magnocellular neurones isolated from the adult rat. *J Physiol* 455: 291–306, 1992.

Oliet SH, **Bourque CW**. Mechanosensitive channels transduce osmosensitivity in supraoptic neurons. *Nature* 364: 341–343, 1993.

Oliet SH, **Bourque CW**. Osmoreception in magnocellular neurosecretory cells: from single channels to secretion. *Trends Neurosci* 17: 340–344, 1994.

Palazzo E, **Luongo L**, **de Novellis V**, **Berrino L**, **Rossi F**, **Maione S**. Moving towards supraspinal TRPV1 receptors for chronic pain relief. *Mol Pain* 6: 66, 2010.

Park SJ, **Haan KD**, **Nakamura Y**, **Fukami K**, **Fisher TE**. PLCδ1 Plays Central Roles in the Osmotic Activation of ΔN-TRPV1 Channels in Mouse Supraoptic Neurons and in Murine Osmoregulation. *J Neurosci* 41: 3579–3587, 2021.

Partridge LD, **Donald Partridge L**, **Partridge LD**. Alteration of Membrane Potential. *Nervous System Actions and Interactions* : 235–259, 2003.

Pastan I, **Willingham MC**. The Pathway of Endocytosis. In: *Endocytosis*, edited by Pastan I, Willingham MC. Boston, MA: Springer US, 1985, p. 1–44.

Petersen MB. The effect of vasopressin and related compounds at V1a and V2 receptors in animal models relevant to human disease. *Basic Clin Pharmacol Toxicol* 99: 96–103, 2006.

Pinarbasi T, **Sozbilir M**, **Canpolat N**. Prospective chemistry teachers' misconceptions about colligative properties: boiling point elevation and freezing point depression. *Chem. Educ. Res. Pract.* 10: 273–280, 2009.

Planells-Cases R, **Ferrer-Montiel A**. TRP Channel Trafficking. In: *TRP Ion Channel Function in Sensory Transduction and Cellular Signaling Cascades*, edited by Liedtke WB, Heller S. Boca Raton (FL): CRC Press/Taylor & Francis, 2011.

Poulain DA, **Wakerley JB**. Electrophysiology of hypothalamic magnocellular neurones secreting oxytocin and vasopressin. *Neuroscience* 7: 773–808, 1982.

Pow DV, **Morris JF**. Differential distribution of acetylcholinesterase activity among vasopressin- and oxytocin-containing supraoptic magnocellular neurons. *Neuroscience* 28: 109–119, 1989.

Prager-Khoutorsky M, **Bourque CW**. Osmosensation in vasopressin neurons: changing actin density to optimize function. *Trends Neurosci* 33: 76–83, 2010.

Prager-Khoutorsky M, **Bourque CW**. Mechanical Basis of Osmosensory Transduction in Magnocellular Neurosecretory Neurones of the Rat Supraoptic Nucleus. *Journal of Neuroendocrinology* 27: 507–515, 2015.

Prager-Khoutorsky M, **Khoutorsky A**, **Bourque CW**. Unique interweaved microtubule scaffold mediates osmosensory transduction via physical interaction with TRPV1. *Neuron* 83: 866–878, 2014.

Prager-Khoutorsky M. Mechanosensing in hypothalamic osmosensory neurons. *Seminars in Cell & Developmental Biology* 71: 13–21, 2017.

Premkumar LS, **Ahern GP**. Induction of vanilloid receptor channel activity by protein kinase C. *Nature* 408: 985–990, 2000.

Premkumar LS, **Sikand P**. TRPV1: a target for next generation analgesics. *Curr Neuropharmacol* 6: 151–163, 2008.

Pryer NK, **Wuestehube LJ**, **Schekman R**. Vesicle-mediated protein sorting. *Annu Rev Biochem* 61: 471–516, 1992.

Qadri F, **Culman J**, **Veltmar A**, **Maas K**, **Rascher W**, **Unger T**. Angiotensin II-induced vasopressin release is mediated through alpha-1 adrenoceptors and angiotensin II AT1 receptors in the supraoptic nucleus. *J Pharmacol Exp Ther* 267: 567–574, 1993.

Qiu D-L, **Shirasaka T**, **Chu C-P**, **Watanabe S**, **Yu N-S**, **Katoh T**, **Kannan H**. Effect of hypertonic saline on rat hypothalamic paraventricular nucleus magnocellular neurons in vitro. *Neuroscience Letters* 355: 117–120, 2004.

Raimondi A, **Ferguson SM**, **Lou X**, **Armbruster M**, **Paradise S**, **Giovedi S**, **Messa M**, **Kono N**, **Takasaki J**, **Cappello V**, **O'Toole E**, **Ryan TA**, **De Camilli P**. Overlapping role of dynamin isoforms in synaptic vesicle endocytosis. *Neuron* 70: 1100–1114, 2011.

Raucher D, **Stauffer T**, **Chen W**, **Shen K**, **Guo S**, **York JD**, **Sheetz MP**, **Meyer T**. Phosphatidylinositol 4,5-Bisphosphate Functions as a Second Messenger that Regulates Cytoskeleton–Plasma Membrane Adhesion. *Cell* 100: 221–228, 2000.

Rebecchi MJ, **Pentyala SN**. Structure, function, and control of phosphoinositide-specific phospholipase C. *Physiol Rev* 80: 1291–1335, 2000.

Renaud LP, **Rogers J**, **Sgro S**. Terminal degeneration in supraoptic nucleus following subfornical organ lesions: ultrastructural observations in the rat. *Brain Res* 275: 365–368, 1983.

Rhee SG. Regulation of phosphoinositide-specific phospholipase C. *Annu Rev Biochem* 70: 281–312, 2001.

Rhoades R, **Bell DR**. *Medical Physiology: Principles for Clinical Medicine*. Wolters Kluwer, 2017.

Robertson GL, **Shelton RL**, **Athar S**. The osmoregulation of vasopressin. *Kidney Int* 10: 25–37, 1976.

Rohacs T, **Thyagarajan B**, **Lukacs V**. Phospholipase C mediated modulation of TRPV1 channels. *Mol Neurobiol* 37: 153–163, 2008.

Rohacs T. Regulation of transient receptor potential channels by the phospholipase C pathway. *Adv Biol Regul* 53: 341–355, 2013.

Rolls BJ, **Phillips PA**. Aging and disturbances of thirst and fluid balance. *Nutr Rev* 48: 137–144, 1990.

Roper P, **Callaway J**, **Armstrong W**. Burst initiation and termination in phasic vasopressin cells of the rat supraoptic nucleus: a combined mathematical, electrical, and calcium fluorescence study. *J Neurosci* 24: 4818–4831, 2004.

Rothman JE. Mechanisms of intracellular protein transport. *Nature* 372: 55–63, 1994.

Sabatini BL, **Regehr WG**. Timing of synaptic transmission. *Annu Rev Physiol* 61: 521–542, 1999.

Sakai H, **Moriura Y**, **Notomi T**, **Kawawaki J**, **Ohnishi K**, **Kuno M**. Phospholipase C-dependent Ca2+-sensing pathways leading to endocytosis and inhibition of the plasma membrane vacuolar H+-ATPase in osteoclasts. *Am J Physiol Cell Physiol* 299: C570–8, 2010.

Sawka MN, **Montain SJ**. Fluid and electrolyte supplementation for exercise heat stress. *Am J Clin Nutr* 72: 564S–72S, 2000.

Segovia M, **Alés E**, **Montes MA**, **Bonifas I**, **Jemal I**, **Lindau M**, **Maximov A**, **Südhof TC**,

Alvarez de Toledo G. Push-and-pull regulation of the fusion pore by synaptotagmin-7. *Proc Natl Acad Sci U S A* 107: 19032–19037, 2010.

Senning EN, **Collins MD**, **Stratiievska A**, **Ufret-Vincenty CA**, **Gordon SE**. Regulation of TRPV1 ion channel by phosphoinositide (4,5)-bisphosphate: the role of membrane asymmetry. *J Biol Chem* 289: 10999–11006, 2014.

Shah L, **Bansal V**, **Rye PL**, **Mumtaz N**, **Taherian A**, **Fisher TE**. Osmotic activation of phospholipase C triggers structural adaptation in osmosensitive rat supraoptic neurons. *The Journal of Physiology* 592: 4165–4175, 2014.

Sharif Naeini R, **Witty M-F**, **Séguéla P**, **Bourque CW**. An N-terminal variant of Trpv1 channel is required for osmosensory transduction. *Nat Neurosci* 9: 93–98, 2006.

Sharif-Naeini R, **Ciura S**, **Stachniak TJ**, **Trudel E**, **Bourque CW**. Neurophysiology of supraoptic neurons in C57/BL mice studied in three acute in vitro preparations. *Prog Brain Res* 170: 229–242, 2008.

Sheehan K, **Lee J**, **Chong J**, **Zavala K**, **Sharma M**, **Philipsen S**, **Maruyama T**, **Xu Z**, **Guan Z**, **Eilers H**, **Kawamata T**, **Schumacher M**. Transcription factor Sp4 is required for hyperalgesic state persistence. *PLoS One* 14: e0211349, 2019.

Shpetner HS, **Vallee RB**. Identification of dynamin, a novel mechanochemical enzyme that mediates interactions between microtubules. *Cell* 59: 421–432, 1989.

Shuster SJ, **Riedl M**, **Li X**, **Vulchanova L**, **Elde R**. Stimulus-dependent translocation of kappa opioid receptors to the plasma membrane. *J Neurosci* 19: 2658–2664, 1999.

Smith D, **Moore K**, **Tormey W**, **Baylis PH**, **Thompson CJ**. Downward resetting of the osmotic threshold for thirst in patients with SIADH. *Am J Physiol Endocrinol Metab* 287: E1019–23, 2004.

Smith RJ, **Sam LM**, **Justen JM**, **Bundy GL**, **Bala GA**, **Bleasdale JE**. Receptor-coupled signal transduction in human polymorphonuclear neutrophils: effects of a novel inhibitor of phospholipase C-dependent processes on cell responsiveness. *J Pharmacol Exp Ther* 253: 688–697, 1990.

Sofroniew MV. Morphology of Vasopressin and Oxytocin Neurones and Their Central and Vascular Projections. *The Neurohypophysis: Structure, Function and Control, Proceedings of the 3rd International Conference on the Neurohypophysis* : 101–114, 1983.

Stern JE, **Armstrong WE**. Reorganization of the dendritic trees of oxytocin and vasopressin neurons of the rat supraoptic nucleus during lactation. *J Neurosci* 18: 841–853, 1998.

Strong JA, **Fox AP**, **Tsien RW**, **Kaczmarek LK**. Stimulation of protein kinase C recruits covert calcium channels in Aplysia bag cell neurons. *Nature* 325: 714–717, 1987.

Studdard PW, **Stein JL**, **Cosentino MJ**. The effects of oxytocin and arginine vasopressin in vitro on epididymal contractility in the rat. *Int J Androl* 25: 65–71, 2002.

Studer M, **McNaughton PA**. Modulation of single-channel properties of TRPV1 by phosphorylation. *J Physiol* 588: 3743–3756, 2010.

Südhof TC. The synaptic vesicle cycle: a cascade of protein–protein interactions. *Nature* 375: 645–653, 1995.

Suh B-C, **Hille B**. PIP2 is a necessary cofactor for ion channel function: how and why? *Annu Rev Biophys* 37: 175–195, 2008.

Suh P-G, **Park J-I**, **Manzoli L**, **Cocco L**, **Peak JC**, **Katan M**, **Fukami K**, **Kataoka T**, **Yun S**, **Ryu SH**. Multiple roles of phosphoinositide-specific phospholipase C isozymes. *BMB Rep* 41: 415–434, 2008.

Suh PG, **Ryu SH**, **Choi WC**, **Lee KY**, **Rhee SG**. Monoclonal antibodies to three phospholipase C isozymes from bovine brain. *J Biol Chem* 263: 14497–14504, 1988.

Swaab DF, **Pool CW**, **Nijveldt F**. Immunofluorescence of vasopressin and oxytocin in the rat hypothalamo-neurohypophyseal system. *J Neural Transm* 36: 195–215, 1975.

Tan NY, **Khachigian LM**. Sp1 phosphorylation and its regulation of gene transcription. *Mol Cell Biol* 29: 2483–2488, 2009.

Tanaka M, **Cummins TR**, **Ishikawa K**, **Black JA**, **Ibata Y**, **Waxman SG**. Molecular and functional remodeling of electrogenic membrane of hypothalamic neurons in response to changes in their input. *Proc Natl Acad Sci U S A* 96: 1088–1093, 1999.

Terry J. The major electrolytes: sodium, potassium, and chloride. *J Intraven Nurs* 17: 240–247, 1994.

Teruel MN, **Meyer T**. Translocation and reversible localization of signaling proteins: a dynamic future for signal transduction. *Cell* 103: 181–184, 2000.

Theodosis DT, **Poulain DA**. Evidence for structural plasticity in the supraoptic nucleus of the rat hypothalamus in relation to gestation and lactation. *Neuroscience* 11: 183–193, 1984.

Thrasher TN, **Keil LC**, **Ramsay DJ**. Lesions of the organum vasculosum of the lamina terminalis (OVLT) attenuate osmotically-induced drinking and vasopressin secretion in the dog. *Endocrinology* 110: 1837–1839, 1982.

Toullec D, **Pianetti P**, **Coste H**, **Bellevergue P**, **Grand-Perret T**, **Ajakane M**, **Baudet V**, **Boissin P**, **Boursier E**, **Loriolle F**. The bisindolylmaleimide GF 109203X is a potent and selective inhibitor of protein kinase C. *J Biol Chem* 266: 15771–15781, 1991.

Tucker VA. Respiratory Exchange and Evaporative Water Loss in the Flying Budgerigar. *J Exp Biol* 48: 67–87, 1968.

Tweedle CD, **Hatton GI**. Ultrastructural comparisons of neurons of supraoptic and circularis nuclei in normal and dehydrated rats. *Brain Res Bull* 1: 103–121, 1976.

Tweedle CD, **Hatton GI**. Ultrastructural changes in rat hypothalamic neurosecretory cells and their associated glia during minimal dehydration and rehydration. *Cell Tissue Res* 181: 59–72, 1977.

Vallis Y, **Wigge P**, **Marks B**, **Evans PR**, **McMahon HT**. Importance of the pleckstrin homology domain of dynamin in clathrin-mediated endocytosis. *Curr Biol* 9: 257–260, 1999.

Vellani V, **Mapplebeck S**, **Moriondo A**, **Davis JB**, **McNaughton PA**. Protein kinase C activation potentiates gating of the vanilloid receptor VR1 by capsaicin, protons, heat and anandamide. *J Physiol* 534: 813–825, 2001.

Verbalis JG, **Drutarosky MD**. Adaptation to chronic hypoosmolality in rats. *Kidney Int* 34: 351–360, 1988.

Verbalis JG, **Mangione MP**, **Stricker EM**. Oxytocin produces natriuresis in rats at physiological plasma concentrations. *Endocrinology* 128: 1317–1322, 1991.

Verney E. TheAntidiuretic Hormone and the Factors Which Determine Its Release. In: *Proc Roy*. date unknown, p. 25–106.

Vieira AV, **Lamaze C**, **Schmid SL**. Control of EGF receptor signaling by clathrin-mediated endocytosis. *Science* 274: 2086–2089, 1996.

Vivona S, **Cipriano DJ**, **O'Leary S**, **Li YH**, **Fenn TD**, **Brunger AT**. Disassembly of all SNARE complexes by N-ethylmaleimide-sensitive factor (NSF) is initiated by a conserved 1:1 interaction between α-soluble NSF attachment protein (SNAP) and SNARE complex. *J Biol Chem* 288: 24984–24991, 2013.

Voet D, **Voet JG**, **Pratt CW**, **Others**. *Fundamentals of biochemistry*. 2000.

Wakerley JB, **Poulain DA**, **Brown D**. Comparison of firing patterns in oxytocin- and vasopressin-releasing neurones during progressive dehydration. *Brain Research* 148: 425–440, 1978.

Wan Q, **Xiong ZG**, **Man HY**, **Ackerley CA**, **Braunton J**, **Lu WY**, **Becker LE**, **MacDonald JF**, **Wang YT**. Recruitment of functional GABAA receptors to postsynaptic domains by insulin. *Nature* 388: 686–690, 1997.

Weisinger RS, **Denton DA**, **McKinley MJ**. Self-administered intravenous infusion of

hypertonic solutions and sodium appetite of sheep. *Behav Neurosci* 97: 433–444, 1983.

Whitnall MH, **Gainer H**, **Cox BM**, **Molineaux CJ**. Dynorphin-A-(1-8) is contained within vasopressin neurosecretory vesicles in rat pituitary. *Science* 222: 1137–1139, 1983.

You H-L, **Eng H-L**, **Hsu S-F**, **Chen C-M**, **Ye T-C**, **Liao W-T**, **Huang M-Y**, **Baer R**, **Cheng J-T**. A PKC-Sp1 signaling pathway induces early differentiation of human keratinocytes through upregulation of TSG101. *Cell Signal* 19: 1201–1211, 2007.

Yue C, **Mutsuga N**, **Verbalis J**, **Gainer H**. Microarray analysis of gene expression in the supraoptic nucleus of normoosmotic and hypoosmotic rats. *Cell Mol Neurobiol* 26: 959–978, 2006.

Zaelzer C, **Hua P**, **Prager-Khoutorsky M**, **Ciura S**, **Voisin DL**, **Liedtke W**, **Bourque CW**. ΔN-TRPV1: A Molecular Co-detector of Body Temperature and Osmotic Stress. *Cell Rep* 13: 23–30, 2015.

Zerbe RL, **Robertson GL**. Osmoregulation of thirst and vasopressin secretion in human subjects: effect of various solutes. *Am J Physiol* 244: E607–14, 1983.

Zhang B, **Glasgow E**, **Murase T**, **Verbalis JG**, **Gainer H**. Chronic hypoosmolality induces a selective decrease in magnocellular neurone soma and nuclear size in the rat hypothalamic supraoptic nucleus. *J Neuroendocrinol* 13: 29–36, 2001.

Zhang W, **Star B**, **W. R. A. K. J. S. Rajapaksha**, **Fisher TE**. Dehydration increases L-type Ca2 current in rat supraoptic neurons. *The Journal of Physiology* 580: 181–193, 2007a.

Zhang X, **Huang J**, **McNaughton PA**. NGF rapidly increases membrane expression of TRPV1 heat-gated ion channels. *EMBO J* 24: 4211–4223, 2005.

Zhang Z, **Bourque CW**. Osmometry in osmosensory neurons. *Nat Neurosci* 6: 1021–1022, 2003.

Zhang Z, **Bourque CW**. Amplification of transducer gain by angiotensin II-mediated enhancement of cortical actin density in osmosensory neurons. *J Neurosci* 28: 9536–9544, 2008.

Zhang Z, **Kindrat AN**, **Sharif-Naeini R**, **Bourque CW**. Actin filaments mediate mechanical gating during osmosensory transduction in rat supraoptic nucleus neurons. *J Neurosci* 27: 4008–4013, 2007b.

Zingg HH, **Lefebvre D**, **Almazan G**. Regulation of vasopressin gene expression in rat hypothalamic neurons. Response to osmotic stimulation. *J Biol Chem* 261: 12956–12959, 1986.

Zorec R. SNARE-mediated vesicle navigation, vesicle anatomy and exocytotic fusion pore. *Cell Calcium* 73: 53–54, 2018.